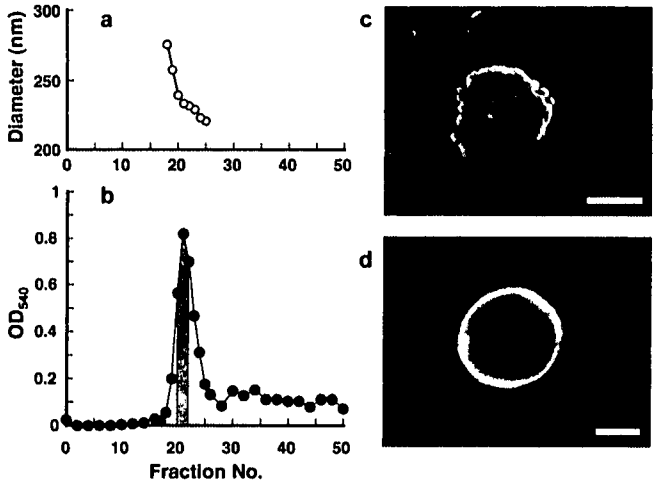

Fig. 1. Purification and Characterization of Recombinant Sendai Virus Particles

SeV-GFP vectors (10 mg protein), partially purified using sucrose step centrifugation, were separated on Sephacryl S1000 columns. The average diameter of the viral particles in each fraction (a) and the optical density (OD) at 540 nm (b) were determined as described in the Materials and Methods. Major peak fractions, indicated by a gray shadow, were collected and used for the perfusion experiment. The average diameter of the viral particles present in this pooled peak fractions was 239.9 nm (polydispersity index 0.083). Recombinant Sendai virus (SeV-EGFP) (c) and naked unilamellar liposomes (d) were fixed with 2.5% glutaraldehyde and trapped on polycarbonate membrane filters (pore size 0.05 μm.). The samples were then dehydrated, dried, coated with osmium and examined as described in the Materials and Methods. Scale bar= 100 nm.

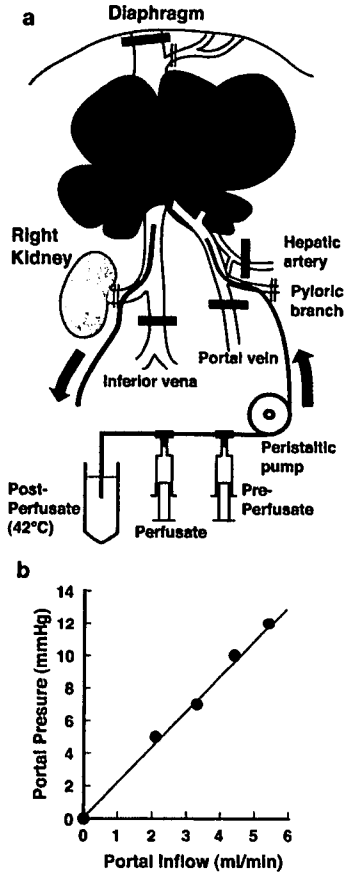

Fig. 2. Portal Pressure Control during Hepatic Perfusion

The distal part of the portal vein, the inferior *vena cava*, the suprahepatic *vena cava* and hepatic artery were clamped just before perfusion as indicated in (a). The preperfusate solution was switched to the perfusate and then to the postperfusate solution using a three-way stopcock. The post perfusate solution was maintained at 42 °C in a water bath. Perfusion inflow was controlled using a peristaltic pump. The relation between the portal inflow and the portal pressure is shown in (b) as the mean of results obtained from two independent experiments.

the particle size distribution of the viruses (data not shown). We also characterized the structure of the recombinant virus using scanning electron microscopy, in comparison with that of the naked liposomes. After the samples had been coated with a 2 nm thick layer of osmium,[25] the viral particle was observed as a microsphere with a complex surface structure and a diameter consistent with that determined by dynamic light scattering (Fig. 1c). On the other hand, the naked unilamellar liposome was observed as a microsphere with a smooth surface (Fig. 1d).

Using these characterized recombinant Sendai virus particles, we optimized the conditions for delivering them by isolated hepatic perfusion in rats. To minimize damage to the hepatic tissue by ischemia, the surgical procedure was arranged to minimize the total perfusion period (Fig. 2a). The animals tolerated the surgical procedure well, without significant irreversible damage in hepatic tissues. One of the key parameters for the successful delivery of Sendai virus vectors by hepatic perfusion is the control of portal pressure. The mean pore size of the hepatic sinusoid is 117 nm (ranging from 40 to 260 nm) under normal portal pressure (7 mmHg).[28] However, the sinusoid is a relatively flexible structure and the mesh size of the sieve can be altered artificially by controlling the portal pressure. Thus, Fraser *et al.* reported that the mean inner diameter of the hepatic sinusoid increases to 193 nm (ranging from 60 to 600 nm) when the vessel is perfused under increased portal pressure (15 mmHg).[28] We controlled portal pressure precisely by regulating the rate of perfusion with a peristaltic pump. As shown in Fig. 2b, we found that the portal pressure correlated linearly with the perfusion rate, from 5 mmHg (average portal pressure of the normal experimental animals) at 2.1 ml/min to 12 mmHg at 5.4 ml/min. We used a portal pressure of 12 mmHg or less, because greater pressure has been defined as clinically significant portal hypertension.[29] We expected that the sinusoids might alter their sieve structure reversibly within this physiological range, allowing the Sendai virus particles to pass through the sieve. Administration under the controlled high pressure is also a key factor in hydrodynamic-based transfection of plasmid DNA through peripheral vein infusion.[30] For example, Zhang *et al.* reported that the efficient plasmid delivery was observed in rats under administration at 24 ml/min,[31] the condition less physiologic compared to our perfusion condition; we could not detect any luciferase activity when 150 μg of pCMV-luc[32] was perfused at 5.4 ml/min (data not shown).

We also optimized the concentration of the vectors in the perfusate to minimize hepatic injury. We first perfused 10^9 plaque-formation units (pfu) of Sendai virus (10^8 pfu/ml in 10 ml) and examined tissue sections prepared 14 h later. As the total number of parenchymal hepatocytes in the rat liver is *ca.* 5×10^8, and as 1 pfu of virus corresponds to about 50 physical viral particles (M. Nakanishi, unpublished observations), this amount of vector should suffice for delivering foreign genes into all the parenchymal hepatocytes. However, perfusion of the vector at 10^8 pfu/ml caused extensive liver necrosis (Fig. 3a). These lesions might have resulted from ischemia caused by microcirculatory dysfunction, because blood clotting in the hepatic vessels was detected in the tissue sections (arrowheads in Fig. 3). As this was not observed

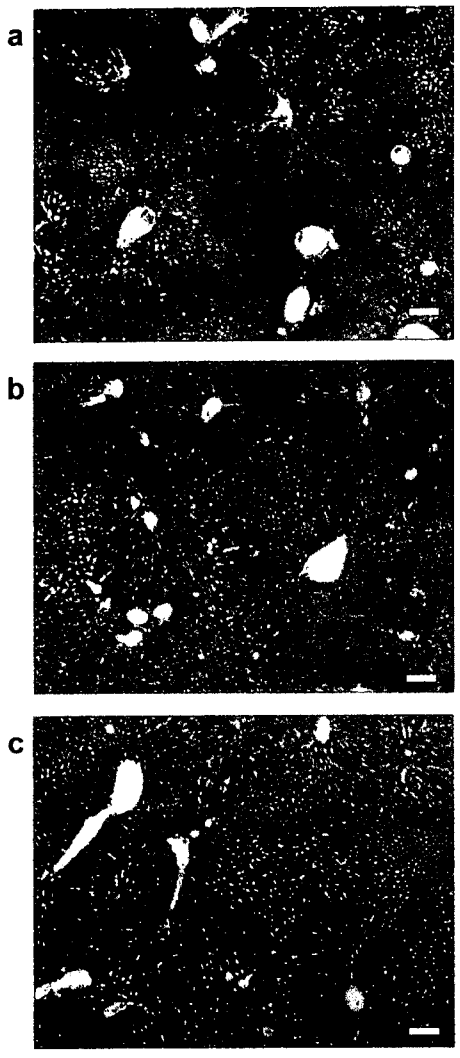

Fig. 3. Histological Analysis of Sections of Hepatic Tissues Perfused Under Various Conditions and Fixed After 14 h

Tissue sections were examined after standard hematoxylin and eosin staining. Perfusion conditions were: perfusion with SeV-EGFP vector at 10^8 pfu/ml and postperfusion at 25 °C (a); perfusion at 10^8 pfu/ml and postperfusion at 42 °C (b); perfusion with 10^7 pfu/ml and postperfusion at 42 °C (c). Arrowheads indicate blood vessels with clotting. Scale bar = 100 nm.

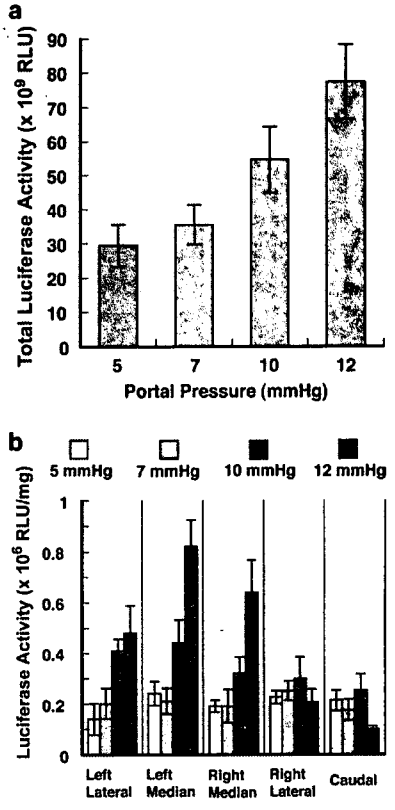

Fig. 4. Luciferase Activity in the Hepatic Tissue Perfused with SeV-luc Vector

SeV-luc (10^8 pfu) was perfused under various portal pressures. After 4 h, the animals were killed and the luciferase activities in the liver were determined as described in the Materials and Methods. Total luciferase activity in hepatic tissue (a) is presented as mean luciferase activities and standard deviations in relative light units (RLU), based on four independent experiments. Specific luciferase activity in each lobe (b) is presented as mean RLU per microgram of protein with standard deviations, based on four independent experiments. Wet weights of the tissues were: left lateral lobe, 3.7±0.4 g; left median lobe, 2.6±0.3 g; right median lobe, 1.1±0.1 g; right lateral lobe, 2.0±0.2 g and caudate lobe, 0.8±0.1 g.

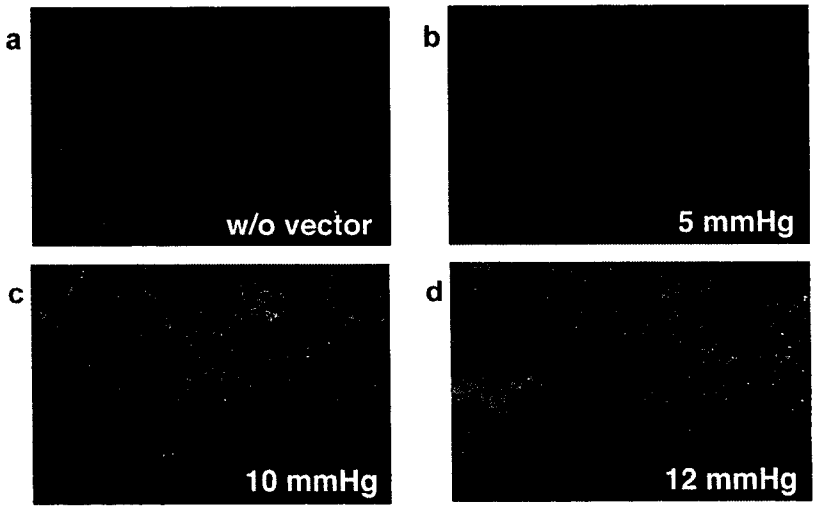

Fig. 5. Levels of Enhanced Green Fluorescent Protein (EGFP) in Hepatic Tissues Perfused with SeV-EGFP Vector (10^7 pfu/ml) at the Following Portal Pressures: 5 mmHg (b), 10 mmHg (c), and 12 mmHg (d)

As a control, lactate-Ringer solution containing no vector was perfused at 12 mmHg in (a). After 12 h, the animals were killed and the expression of EGFP in the right median lobe was examined as described in Materials and Methods.

in the tissue samples perfused without viral particles (data not shown), we believe that the viral particles, or the viral envelope proteins on the vessel surface, entrapped the blood cells just after recirculation to cause clotting. However, extensive postperfusion at 25 °C could not prevent these lesions (data not shown). Perfusion at lower temperatures is desirable to avoid hepatic dysfunction and to maintain the biological function of the vectors in the perfusate,[33] whereas incubation at a higher temperature is essential for stimulating virus-induced membrane fusion[34] and for the rapid clearance of the viral glycoproteins from the cell surface.[35] Therefore, we examined the effect of a brief hyperthermic postperfusion (42 °C for 5 min) and found that this procedure largely prevented the formation of necrotic lesions (Fig. 3b).

We also identified vector concentration as another key factor affecting the hepatic lesion: decreasing the vector concentration to 10^7 pfu/ml reduced the rate of formation of hepatic lesions significantly (data not shown). The combination of a perfusion at lower vector concentration (10^7 pfu/ml) with hyperthermic postperfusion (42 °C for 5 min) prevented these necrotic lesions almost completely (Fig. 3c). Therefore, we used these conditions in the subsequent gene transfer experiments.

Using the isolated hepatic perfusion procedures optimized above, we characterized marker gene expression induced by the recombinant Sendai virus vectors expressing luciferase (SeV-luc) and enhanced green fluorescent protein (SeV-EGFP). First, we examined the effect of portal pressure on the luciferase activity in the hepatic tissue into which 10^8 pfu (10^7 pfu/ml in 10 ml) of the SeV-luc vectors had been perfused under various portal pressures. As shown in Fig. 4a, total luciferase activity recovered from the whole liver tissue increased to 260% when the portal pressure during the perfusion was increased from 5 to 12 mmHg. Significant enhancement of gene expression was observed in three upper lobes (the right median lobe, the left median lobe and the left lateral lobe) and the specific luciferase activity (relative light units per microgram of protein) in these lobes increased to 340% (Fig. 4b). These three lobes, corresponding to 73% of the total liver mass, expressed 92% of the total luciferase activity at a portal pressure of 12 mmHg. On the other hand, luciferase activities in the lower lobes did not respond to this portal pressure significantly (Fig. 4b). Thus, at least in the upper major lobes, a moderate portal pressure (12 mmHg) enhanced the delivery of the vectors across the sinusoid barrier into the hepatic tissues. This observed unevenness in gene expression may be caused by inevitable technical difficulty of the surgical procedure in small animals; de Roos *et al.* reported that the trans-gene expression varied significantly (up to 1000-fold) among experiments when adenovirus vectors were administrated by isolated liver perfusion.[15]

Next, we examined the effect of portal pressure on the spatial distribution of the cells expressing the marker genes in the hepatic tissue. We delivered 10^8 pfu (10^7 pfu/ml in 10 ml) of the SeV-EGFP vectors by perfusion under various portal pressures, then fixed the livers and examined the expression of EGFP in frozen sections using fluorescent microscopy (Fig. 5). When the vectors were delivered at the normal portal pressure (5 mmHg), the expression of EGFP was restricted to the endothelium of the hepatic vessels (Fig. 5b).

Table 1. Tissue Distribution of Luciferase Activity in Animals into Which SeV-luc Was Administered by Isolated Hepatic Perfusion

	Luciferase activity (10^9RLU/tissue)						
	Liver	Heart	Lung	Kidney	Spleen	Testis	Thymus
5 mm Hg	11.3±2.7	<0.01	<0.01	<0.01	<0.01	<0.01	<0.01
7 mm Hg	13.1±2.5	<0.01	<0.01	<0.01	<0.01	<0.01	<0.01
10 mm Hg	19.5±4.0	<0.01	<0.01	<0.01	<0.01	<0.01	<0.01
12 mm Hg	27.6±3.3	<0.01	<0.01	<0.01	<0.01	<0.01	<0.01

SeV-pluc (10^8pfu) was perfused under the portal pressures indicated. After 4 h, the animals were killed and the total luciferase activity in each tissue was determined as described in Materials and Methods. The data are presented as means and standard deviations of luciferase activity in relative light units (RLU), based on four animals. <0.01 indicates that the luciferase activity was below the detection limit.

This observation is consistent with the hypothesis that normal hepatic sinusoids prevent the effective access of particles larger than 100 nm in diameter to the parenchymal hepatocytes. However, as the portal pressure was increased, EGFP became detectable in hepatocytes distant from the hepatic vessels (Fig. 5c), and almost all the parenchymal hepatocytes expressed EGFP at the portal pressure of 12 mmHg (Fig. 5d). Increased EGFP expression in the parenchymal hepatocytes was observed in the right median lobe (Fig. 5) as well as in the caudate lobe (data not shown). Thus, a moderate portal pressure of 12 mmHg was sufficient to deliver the Sendai virus-based vectors across the hepatic sinusoid sieve.

We then examined the effectiveness of isolated hepatic perfusion in preventing gene delivery to nonhepatic tissues. We perfused 10^8 pfu of the SeV-luc vector through the portal vein, and examined luciferase activities in hepatic and nonhepatic tissues. As shown in Table 1, activities in nonhepatic tissues (heart, lung, left kidney, spleen, testis and thymus) were below the detection limit, regardless of the perfusion rate (portal pressure), whereas the hepatic tissue expressed this enzyme at least 1000 times greater that of the nonhepatic tissues. We also perfused 10^8 pfu of the SeV-EGFP vectors through the portal vein at 12 mmHg, and found no EGFP-positive cells in nonhepatic tissues examined as above (data not shown). Therefore, we conclude that our perfusion protocol is an effective approach for targeting gene delivery vectors to the hepatic tissues and for preventing undesired systemic vector delivery.

DISCUSSION

Although the liver is one of the major target organs for gene therapy of inheriting metabolic disorders, no practical strategy has been established yet that achieves continuous supplement of therapeutic gene products in this organ. This is partly due to the limitations of current gene transfer vectors that persistent expression of therapeutic genes requires their integration into the host chromosome. Plasmid DNA and adenovirus vectors are not considered as practical candidates in liver-targeted gene therapy because they usually could not insert genes into the host chromosome. Retrovirus, lentivirus- and AAV-vectors can integrate their genome into the host chromosomes, but with low efficiency in nondividing tissue cells (including hepatocytes). Even if we can facilitate random gene integration dramatically, it may cause severe side effects (oncogenesis) instead, as revealed in re-

cent clinical trials using bone-marrow stem cells.

In this context, the Sendai virus vector is unique among the current vector systems. It transcribes mRNA from the cytoplasmic RNA genome, which avoids the possible side effects caused by the random gene integration. Furthermore, we recently develop a novel Sendai virus vector based on a variant virus strain, capable of sustained gene expression without chromosomal integration. By using this novel vector, we observed that strong marker gene expression has been sustained for more than six months in cultured cells without obvious cytotoxicity (Nishimura and Nakanishi, manuscript in preparation). These characteristics strongly suggest that this novel Sendai virus-based vector will becomes a candidate tool for gene therapy targeted to the liver. Nevertheless, application of the Sendai virus vector is limited due to the absence of the appropriate protocol of administration to the liver.

The primary objective of this article is to demonstrate a novel and practical protocol for administrating the recombinant Sendai virus vectors into the liver *in situ*. As the sizes and structures of the various Sendai virus vectors are essentially same regardless their genetic structures, the procedure described in this article is also applicable to the improved vectors. Our isolated hepatic perfusion procedure provides for the first time a protocol for administering Sendai virus vectors efficiently into hepatic tissues *in situ*. Moreover, we have proved that this procedure effectively avoids the delivery of foreign genes into nonhepatic tissues, in particular the gonads. The ethical guidelines for gene therapy prohibit the delivery of foreign genes into the reproductive organs (testis and ovary) and germ cell lineage.[36] Moreover, ectopic unregulated expression of therapeutic genes may cause unexpected side effects. Therefore, delivering the vectors to appropriate target organs and tissues, and restricting the expression of the therapeutic genes to these target sites are fundamental issues for *in vivo* gene therapy.

The vectors we used in this study are prototype Sendai virus vectors retaining full function of viral replication. These vectors are ready to prepare in large-scale and are suitable for examining transient (but strong) gene expression *in situ*. However, due to the death by viremia, they are not suitable for examining the time course of gene expression and for evaluating therapeutic effect of the gene products. This forced us to assay gene expression in the early stage after administration (at 4 h for luciferase and at 12 h for EGFP), thus made it difficult to compare the gene expression with other system. This failure was not due to the surgical procedure but reflected the characteristics of the prototype vector, because all the animals perfused with UV-inactivated virus survived without symptom of the hepatic failure (data not shown). Currently, we are investigating the procedure for large-scale production of novel improved Sendai virus vectors, and will examine their effectiveness using the isolated perfusion protocol described in this article.

Although the hepatic perfusion is not yet established as a standard clinical procedure, regional high-dose administration of melpharan *via* isolated hepatic perfusion was effective for treating nonresectable hepatic metastatic tumors in several clinical trials.[12,13] The morbidity of the operation was reported to be acceptably low in a recent clinical trial for treating patients with nonresectable hepatic metastases of colorectal cancer (2%, or one perioperative death in 50 patients),[37] suggesting that this procedure may become a practical procedure for gene therapy. Therefore, successful hepatic delivery of improved recombinant Sendai viruses promises to become an important step for gene therapy of metabolic diseases.

Acknowledgments This work was partly supported by grants (to M. N.) from the Ministry of Education, Culture, Sports, Science and Technology of Japan and from the Ministry of Health and Welfare of Japan.

REFERENCES

1) Lamb R. A., Kolakofsky D., "Fundamental Virology, Fourth Edition," ed. by Knipe D. M., Howley P. M., Lippincott Williams & Wilkins, Philadelphia, Pennsylvania, U.S.A., 2001, pp. 689—724.
2) Griesenbach U., Cassady R. L., Ferrari S., Fukumura M., Muller C., Schmitt E., Zhu J., Jeffery P. K., Nagai Y., Geddes D. M., Hasegawa M., Alton E. W., *Mol. Ther.*, **5**, 98—103 (2002).
3) Inoue M., Tokusumi Y., Ban H., Shirakura M., Kanaya T., Yoshizaki M., Hironaka T., Nagai Y., Iida A., Hasegawa M., *J. Gene Med.*, **6**, 1069—1081 (2004).
4) Nakanishi M., Mizuguchi H., Ashihara K., Senda T., Akuta T., Okabe J., Nagoshi E., Masago A., Eguchi A., Suzuki Y., Inokuchi H., Watabe A., Ueda S., Hayakawa T., Mayumi T., *J. Cont. Rel.*, **54**, 61—68 (1998).
5) Yonemitsu Y., Kitson C., Ferrari S., Farley R., Griesenbach U., Judd D., Steel R., Scheid P., Zhu J., Jeffery P. K., Kato A., Hasan M. K., Nagai Y., Masaki I., Fukumura M., Hasegawa M., Geddes D. M., Alton E. W., *Nat. Biotechnol.*, **18**, 970—973 (2000).
6) Masaki I., Yonemitsu Y., Komori K., Ueno H., Nakashima Y., Nakagawa K., Fukumura M., Kato A., Hasan M. K., Nagai Y., Sugimachi K., Hasegawa M., Sueishi K., *FASEB J.*, **15**, 1294—1296 (2001).
7) Shiotani A., Fukumura M., Maeda M., Hou X., Inoue M., Kanamori, T., Komaba S., Washizawa K., Fujikawa S., Yamamoto T., Kadono C., Watabe K., Fukuda H., Saito K., Sakai Y., Nagai Y., Kanzaki J., Hasegawa M., *Gene Ther.*, **8**, 1043—1050 (2001).
8) Ikeda Y., Yonemitsu Y., Sakamoto T., Ishibashi T., Ueno H., Kato A., Nagai Y., Fukumura M., Inomata H., Hasegawa M., Sueishi K., *Exp. Eye Res.*, **75**, 39—48 (2002).
9) Li H. O., Zhu Y. F., Asakawa M., Kuma H., Hirata T., Ueda Y., Lee Y. S., Fukumura M., Iida A., Kato A., Nagai Y., Hasegawa M., *J. Virol.*, **74**, 6564—6569 (2000).
10) Okada Y., *Methods Enzymol.*, **221**, 18—41 (1993).
11) Fraser R., Dobbs B. R., Rogers G. W., *Hepatology*, **21**, 863—874 (1995).
12) Elaraj D. M., Alexander H. R., *Cancer J.*, **10**, 128—138 (2004).
13) Rothbarth J., Tollenaar R. A., Schellens J. H., Nortier J. W., Kool L. J., Kuppen P. J., Mulder G. J., van de Velde C. J., *Eur. J. Cancer*, **40**, 1812—1824 (2004).
14) Brooks A. D., Ng B., Liu D., Brownlee M., Burt M., Federoff H. J., Fong Y., *Surgery*, **129**, 324—334 (2001).
15) de Roos W. K., Fallaux F. J., Marinelli A. W., Lazaris-Karatzas A., von Geusau A. B., van der Eb M. M., Cramer S. J., Terpstra O. T., Hoeben R. C., *Gene Ther.*, **4**, 55—62 (1997).
16) Olthoff K. M., Judge T. A., Gelman A. E., da Shen X., Hancock W. W., Turka L. A., Shaked A., *Nat. Med.*, **4**, 194—200 (1998).
17) Shiraishi M., Nagahama M., Obuchi Y., Taira K., Tomori H., Sugawa H., Kusano T., Muto Y., *J. Surg. Res.*, **76**, 105—110 (1998).
18) Hasan M. K., Kato A., Shioda T., Sakai Y., Yu D., Nagai Y., *J. Gen. Virol.*, **78**, 2813—2820 (1997).
19) Agungpriyono D. R., Yamaguchi R., Uchida K., Tohya Y., Kato A., Nagai Y., Asakawa M., Tateyama S., *J. Vet. Med. Sci.*, **62**, 223—228 (2000).
20) Nakanishi M., Uchida T., Sugawa H., Ishiura M., Okada Y., *Exp. Cell Res.*, **159**, 399—409 (1985).
21) Kato K., Nakanishi M., Kaneda Y., Uchida T., Okada Y., *J. Biol. Chem.*, **266**, 3361—3364 (1991).
22) Reynolds J. A., Nozaki Y., Tanford C., *Anal. Biochem.*, **130**, 471—474 (1983).

23) Harada A., Kataoka K., *Macromolecules*, **36**, 4995—5001 (2003).
24) Sugita K., Maru M., Sato K., *Jpn. J. Microbiol.*, **18**, 262—264 (1974).
25) Sasaki K., Johkura K., Ogiwara N., Liang Y., Cui L., Teng R., Okouchi Y., Asanuma K., Ishida O., Maruyama K., *Cryobiology*, **42**, 145—150 (2001).
26) Eguchi A., Akuta T., Okuyama H., Senda T., Yokoi H., Inokuchi H., Fujita S., Hayakawa T., Takeda K., Hasegawa M., Nakanishi M., *J. Biol. Chem.*, **276**, 26204—26210 (2001).
27) Hosaka Y., Kitano H., Ikeguchi S., *Virology*, **29**, 205—221 (1966).
28) Fraser R., Bowler L. M., Day W. A., Dobbs B., Johnson H. D., Lee D., *Br. J. Exp. Pathol.*, **61**, 222—228 (1980).
29) Thalheimer U., Mela M., Patch D., Burroughs A. K., *Hepatology*, **39**, 286—290 (2004).
30) Liu F., Song Y., Liu D., *Gene Ther.*, **6**, 1258—1266 (1999).
31) Zhang X., Dong X., Sawyer G. J., Collins L., Fabre J. W., *J. Gene Med.*, **6**, 693—703 (2004).
32) Akuta T., Eguchi A., Okuyama H., Senda T., Inokuchi H., Suzuki Y., Nagoshi E., Mizuguchi H., Hayakawa T., Takeda K., Hasegawa M., Nakanishi M., *Biochem. Biophys. Res. Commun.*, **297**, 779—786 (2002).
33) Okada Y., Tadokoro J., *Exp. Cell Res.*, **26**, 108—118 (1962).
34) Kim J., Okada Y., *Exp. Cell Res.*, **132**, 125—136 (1981).
35) Kim J., Okada Y., *Exp. Cell Res.*, **140**, 127—136 (1982).
36) Juengst E. T., Walters L., "The Development of Human Gene Therapy," ed. by Friedmann T., Cold Spring Harbor Laboratory Press, Cold Spring Harbor, New York, U.S.A., 1999, pp. 691—712.
37) Bartlett D. L., Libutti S. K., Figg W. D., Fraker D. L., Alexander H. R., *Surgery*, **129**, 176—187 (2001).

THE JOURNAL OF GENE MEDICINE
J Gene Med 2006; 8: 1151–1159.
Published online 14 July 2006 in Wiley InterScience (www.interscience.wiley.com) DOI: 10.1002/jgm.938

RESEARCH ARTICLE

Naked Sendai virus vector lacking all of the envelope-related genes: reduced cytopathogenicity and immunogenicity

Mariko Yoshizaki[1]
Takashi Hironaka[1]
Hitoshi Iwasaki[1]
Hiroshi Ban[1]
Yumiko Tokusumi[1]
Akihiro Iida[1]
Yoshiyuki Nagai[2]
Mamoru Hasegawa[1]
Makoto Inoue[1]*

[1]*DNAVEC Corporation, 1-25-11 Kannondai, Tsukuba-shi, Ibaraki 305-0856, Japan*

[2]*RIKEN, Center of Research Network for Infectious Diseases, 1-7-1 Yuraku-cho, Chiyoda-ku, Tokyo 100-0006, Japan*

*Correspondence to: Makoto Inoue, DNAVEC Corporation, 1-25-11 Kannondai, Tsukuba-shi, Ibaraki 305-0856, Japan.
E-mail: inoue@dnavec-corp.com

Received: 19 December 2005
Revised: 17 March 2006
Accepted: 10 April 2006

Abstract

Background Sendai virus (SeV) is a new class of cytoplasmic RNA vector that is free from genotoxicity that infects and multiplies in most mammalian cells, and directs high-level transgene expression. We improved the vector by deleting all of the envelope-related genes from the SeV genome and thus reducing its immunogenicity.

Methods The matrix (M), fusion (F) and hemagglutinin-neuraminidase (HN) genes-deleted SeV vector (SeV/ΔMΔFΔHN) was recovered in a newly established packaging cell line. Then, the generated SeV/ΔMΔFΔHN vector was characterised by comparing with single gene-deleted type SeV vectors.

Results This SeV/ΔMΔFΔHN vector carrying the green fluorescent protein gene in place of the envelope-related genes could be propagated to a titer of more than 10^8 cell infectious units/ml. This vector showed an efficient transduction capability *in vitro* and *in vivo*, and the cytopathic effect and induction of neutralizing antibody *in vivo* were greatly reduced compared with those of single gene-deleted type SeV vectors. No activity of neutralizing antibody or anti-HN antibody was seen when SeV/ΔMΔFΔHN was transduced *ex vivo*. Additional introduction of amino acid mutations that had been identified from SeV strains causing persistent infections was also effective for the reduction of cytopathic effects.

Conclusions The deletion of genes from the SeV genome and the additional mutation are very effective for reducing both the immunogenic and cytopathic reactions to the SeV vector. These modifications are expected to improve the safety and broaden the range of clinical applications of this new class of cytoplasmic RNA vector. Copyright © 2006 John Wiley & Sons, Ltd.

Keywords Sendai virus; cytoplasmic RNA vector; gene deletion; reduced cytotoxicity; genotoxicity-free; gene therapy

Introduction

A new class of cytoplasmic RNA vectors is thought to provide advanced transgene expression systems that can overcome recent problems of genetic disturbance caused by presently available vectors. The Sendai virus (SeV) vector, based on SeV (belonging to the genus *Respirovirus* of the family *Paramyxoviridae*), infects and multiplies in most mammalian cells, and directs high-level transgene expression. Its replication is independent of nuclear

functions, and there is no DNA phase during its life cycle, so that the possible transformation of cells due to the integration of vector materials into the cellular genome is not a concern [1]. These properties make SeV vectors very promising for applications to gene therapy (cytoplasmic gene therapy) and vaccination via the expression of therapeutic genes and antigens [2,3]. In particular, a clinical trial protocol for therapeutic induction of angiogenesis, which is for the treatment of critical limb ischemia using an SeV vector carrying the fibroblast growth factor-2 gene [4,5], has been approved by the Ministry of Health, Labour and Welfare (MHLW) of Japan and will begin soon. In addition, cancer treatments including treatments for brain tumors [6] and many types of aggressive tumors [7], and a variety of vaccination protocols such as for the human immunodeficiency virus [8,9], using SeV vectors are planned.

The viral envelope comprises a lipid bilayer derived from the host plasma membrane and two inserted viral glycoproteins, fusion (F) and hemagglutinin-neuraminidase (HN) proteins. Beneath the envelope is a lining consisting of the matrix or membrane (M) protein. The F and HN proteins are primarily required during the entry of SeV into cells. The F protein is involved in virus penetration, hemolysis and cell fusion [10]. The HN protein mediates the viral attachment to cells by interacting with cell-surface sialic acid containing receptor(s). The HN protein is known to be one of the major targets of the host humoral immune responses against SeV infection, and to induce NK and cytotoxic T lymphocyte responses [11,12]. The M protein promotes vesiculation of the membrane and the release of particles into the extracellular medium without the aid of other viral proteins [13,14]. We previously succeeded in the recovery of high titers of F-gene-deleted (SeV/ΔF) [15], M-gene-deleted (SeV/ΔM) [16], HN-gene-deleted (SeV/ΔHN), and both M- and F-genes-deleted (SeV/ΔMΔF) [17] SeV vectors in addition to other types of SeV vectors [18] by using packaging cell lines that express the respective proteins encoded by the deleted gene(s). All the vectors showed efficient infectivity and transgene expression in various types of cell lines and primary cells *in vitro*. Deletion of the F gene made the SeV vector non-transmissible, deletion of the M gene worked well to render the vector incapable of directing the formation of particles in infected cells, and deletion of the HN gene was expected to reduce the host immune response against the SeV vector. The single-gene-deleted SeV vectors were also rescued and propagated by another group [19], but multiple-genes-deleted SeV vectors have not been propagated at high titer. For the wide-range application of SeV vectors, such as for the treatment of chronic diseases, virus-gene-derived protein expression should be reduced as much as possible. High-level transgene expression from the SeV vector results from the high-level transcription associated with the genome replication that is directed by nucleoprotein (NP), phospho (P) and large (L) proteins [20]. To keep the high-level expression of SeV vectors, the NP, P and L genes should not be removed. Therefore, the most advanced SeV vector, which reduces the viral genome as much as possible, is the M-, F- and HN-genes-deleted SeV vector (SeV/ΔMΔFΔHN) at present. However, the recovery of SeV/ΔMΔFΔHN has hitherto been very difficult because the efficient complementation of all three proteins (M, F and HN) needed to form the virion particle was essential for its propagation.

In this study, we succeeded in the establishment of a packaging cell line that expresses all three envelope proteins, M, F and HN, by using a Cre/*lox*P induction system. Using this cell line, we succeeded in producing the SeV vector deleted for the M, F and HN genes at a titer of more than 10^8 cell infectious units (CIU)/ml. SeV/ΔMΔFΔHN possesses only the NP, P and L genes in its genome. This vector showed efficient transduction capability and reduced cytopathic effect. Importantly, the immune reaction against SeV was also reduced when SeV/ΔMΔFΔHN was used *in vivo* and *ex vivo*.

Materials and methods

Cells and viruses

Monkey kidney cell lines, LLC-MK_2 and CV-1, were maintained in monolayer cultures in minimal essential medium (MEM) (Invitrogen) supplemented with 10% fetal bovine serum and penicillin-streptomycin in the presence of 5% CO_2. The molecular clone of SeV Z strain with attenuated virulence was used as the starting material for genome modifications in this study. The F, M or both M/F gene(s)-deleted SeV vectors were prepared by using LLC-MK_2 cells stably transformed with the F gene (LLC-MK2/F7 [15], M gene (LLC-MK2/F7/M62 [16]), or both M and F genes (LLC-MK2/F7/M#33 [17]). The SeV/ΔMΔFΔHN was prepared in a new packaging cell line (LLC-MK2/F7/M#33/A/HN7; this report). An adenovirus vector, AxCANCre [21], expressing Cre recombinase, was used for the induction of respective protein(s) encoded by these deleted gene(s).

Plasmid construction

For the construction of genomic cDNA of M-, F- and HN-genes-deleted SeV carrying the green fluorescent protein (GFP) gene, LitmusSalINheIhfrag-ΔMΔFGFP that was used to generate the cDNA of SeV/ΔMΔF-GFP (pSeV/ΔMΔF-GFP) containing the GFP and HN genes in the *Sal* I/*Nhe* I site in LITMUS38 (NEB) [17] was utilised. Inverse polymerase chain reaction (PCR) was conducted with primer pairs of 5′-GAGGTCGCGCGTTAATTAAGCTTTCACCTCAAACAAGC-ACAGATCATGG-3′ and 5′-GCATGTTTCCCAAGGGGAGA-GTTAATTAACCAAGCACTCACAAGGGAC-3′ to introduce the *Pac* I site just behind the P gene. The PCR product was digested with *Pac* I and *Dpn* I and then self-ligated; thus both GFP and HN genes were deleted from LitmusSalINheIhfrag-ΔMΔFGFP and generated

DOI: 10.1002/jgm

LitmusSalINhelhfrag-ΔMΔFΔHN-Pac I. To insert the GFP gene with end and start signals (EIS) between the P and L genes, PCR was conducted with primer pairs of 5′-CTGCGATCGCGCCCCAAGCAGACACCACCT-3′ and 5′-TACGCGATCGCTGATAATGGTCGTGATCAT-3′ on pSeV18+/ΔF-GFP [15] as a template. The amplified GFP fragment was digested with *Sgf* I and inserted into the *Pac* I site of LitmusSalINhelhfrag-ΔMΔFΔHN-PacI to generate LitmusSalINhelhfrag-ΔMΔFΔHN-GFP. The 5.9 kb *Sal* I- and *Nhe* I-digested fragment containing the GFP gene was substituted for the corresponding fragment of pSeV18+/ΔMΔF-GFP to generate pSeV/ΔMΔFΔHN-GFP. To introduce the mutations of persistent infection into the P and L genes, site-directed mutagenesis was conducted using a QuickChange site-directed mutagenesis kit (Stratagene) with the primer pairs 5′-ctcaaacgcatcacgtctcTtTccctccaaagagaagc-3′ (sense) and 5′-gcttctctttggagggAaAgagacgtgatgcgtttgag-3′ (antisense) for L511F in the P gene, and 5′-gttctatcttcctgacTCtatagacctggacacgcttac-3′ (sense) and 5′-gtaagcgtgtccaggtctataGAgtcaggaagatagaac-3′ (antisense) for N1197S and 5′-ctacctattgagcccctttagttgacGaAgataaagataggcta-3′ (sense) and 5′-tagcctatctttatcTtCgtcaactaaggggctcaataggtag-3′ (antisense) for K1795E in the L gene used on pSeV/ΔMΔFΔHN-GFP as a template. Thus, full-length genomic cDNA of pSeV/PLmutΔMΔFΔHN-GFP was generated and its structure was confirmed by sequencing. For the plasmid expressing the HN protein under the control of the *Cre/lox*P induction system [22] a PCR-generated 1.8 kb fragment containing the HN gene from SeV cDNA was inserted into the *Swa* I site of pCALNdLw [22] to generate pCALNdLw/HN, in which the HN gene was located after the drug-resistant gene sandwiched between *lox*P sequences. Hence, the expression of the HN protein in pCALNdLw/HN-introduced cells, LLC-MK2/F7/M#33/A/HN7, was induced after expressing Cre recombinase from AxCANCre.

Insertion of the SEAP gene

To quantify the expression of a foreign gene carried in the SeV genome, the gene for the secreted form of human placental alkaline phosphatase (SEAP) was inserted upstream of the open reading frame of the NP gene. The SEAP gene with the EIS element [17] was introduced into the *Not* I site located in the non-coding sequence between the start (S) signal and the translation initiation codon (ATG) of the NP gene of pSeV/PLmutΔMΔFΔHN-GFP to generate pSeV^{18+}SEAP/PLmutΔMΔFΔHN-GFP.

Cloning and analysis of packaging cell lines

LLC-MK$_2$/F7/M#33 cells were transfected with pCALNdLw/HN using LipofectAMINE PLUS reagent (Invitrogen) according to the manufacturer's instruction. Two weeks after transfection, viable clones of single cell origin in 96-well plates were expanded in 12-well plates, and, when they reached a nearly confluent state, they were infected with AxCANCre at an multiplicity of infection (MOI) of 5 [21,22]. After culturing for 2 days at 32 °C, the cells were recovered and subjected to semiquantitative Western blotting with anti-HN antibody according to a method described previously [16].

M-, F- and HN-genes-deleted SeV vector recovery from cDNA

Preparation of cell lysate containing RNPs and primary virions of SeV/ΔMΔFΔHN-GFP was carried out according to the method described previously [16] with minor modification. Briefly, approximately 1×10^7 LLC-MK$_2$ cells seeded in Ø10-cm dish were transfected with pSeV/ΔMΔFΔHN-GFP and pCAG-plasmids each carrying the NP, P, M, F, HN or L gene (Ban *et al.*, personal communication). The cells were cultured in MEM containing trypsin (7.5 μg/ml). Twenty-four hours after transfection, the cells were overlaid with LLC-MK2/F7/M#33/HN7 cells after induction of M, F and HN proteins by AxCANCre infection at an MOI of 5 and cultured for another 48 h. The cells were harvested and lysed by repeating a freeze/thaw cycle three times in Opti-MEM (Invitrogen). The cell lysate was infected into new LLC-MK2/F7/M#33/HN7 cells after AxCANCre infection. After that, these cells were cultured at 32 °C in MEM containing trypsin for 10 to 20 days. When spread of GFP expression to neighbour cells was seen by fluorescence microscopy, it was considered that viral vectors were recovered in the culture supernatants. Those viral vectors were further amplified by several rounds of propagation. Titers were determined by the proportion of GFP-expressing cells (GFP-CIU) per milliliter [15]. The culture supernatant of the fourth passage was collected and stored at −80 °C, after adding bovine serum albumin (BSA) solution to a final concentration of 1% (w/v), until usage in all the experiments described below.

RT-PCR

Total viral RNA from SeV/ΔMΔFΔHN-GFP was extracted from the supernatant containing viral particles using a QIAamp viral RNA minikit (Qiagen). Reverse-transcription (RT)-PCR was performed in a one-step process using the Superscript RT-PCR system (Invitrogen). RT-PCR amplication was performed with random hexamers and the primer pair 5′-AGAGAACAAGACTAAGGCTACC-3′ (forward primer specific for the P gene) and 5′-TATTCAACCAAAGATCCTGGAACCC-3′ (reverse primer specific for the L gene) probed.

Detection of viral proteins by Western blotting

Analysis of viral proteins by sodium dodecyl sulfate/polyacrylamide gel electrophoresis (SDS-PAGE) was

DOI: 10.1002/jgm

performed according to the method described previously [16]. LLC-MK_2 cells (1×10^6) in 6-well plates were infected at an MOI of 3 with SeV/ΔF-GFP, SeV/ΔM-GFP, SeV/ΔMΔF-GFP or SeV/ΔMΔFΔHN-GFP and incubated in serum-free MEM at 37 °C. Three days after transduction, the cells were recovered and solubilized in a sample buffer (Biolabs) for SDS-PAGE. Proteins separated by SDS-PAGE were transferred to Immobilon-PVDF membranes (Millipore). The membranes were probed with a rabbit polyclonal anti-M antibody [16] or mouse monoclonal anti-F, γ236 [23], and anti-HN, HN-2 [24], antibodies. Secondary antibodies were goat anti-rabbit IgG (Santa Cruz Biotechnology) or goat anti-mouse IgG+IgM (Bioscience) conjugated with horseradish peroxidase. The protein bands were detected by chemiluminescence using ECL Western blotting detection reagents (Amersham Biosciences) following the manufacturer's protocol.

Quantitative analysis of cytotoxicity

Confluent CV-1 cells grown in 96-well plates were infected at an MOI of 0.1, 0.3, 1, 3, 10 or 30 with SeV/ΔF-GFP, SeV/ΔM-GFP, SeV/ΔMΔF-GFP, SeV/ΔMΔFΔHN-GFP or SeV/PLmutΔMΔFΔHN-GFP and incubated at 37 °C in serum-free MEM. The culture supernatants were collected 3 days after transduction and assayed with a cytotoxicity detection kit (Roche) that measures lactase dehydrogenase (LDH) activity released from damaged cells [25].

SEAP assay

Confluent LLC-MK_2 cells grown in 96-well plates were infected at an MOI of 3 with SeV^{18+}SEAP/ΔF-GFP, SeV^{18+}SEAP/ΔMΔF-GFP or SeV^{18+}SEAP/PLmutΔMΔF-ΔHN-GFP and incubated in serum-free MEM at 37 °C. The culture supernatants were collected every 24 h and assayed for SEAP activities using an SEAP reporter assay kit (Toyobo) with an LAS 1000 image analyser (Fuji Film). Means were calculated from three replicate samples.

In vivo study of M-, F- and HN-genes-deleted SeV vector

Twelve BALB/cA mice (Charles River), 7 weeks old weighing 20–25 g, were used. In half of the mice, submandibular lymph nodes (SMLN) were removed before injection. Mice were anaesthetised with diethyl ether, and 5 μl of SeV/ΔF-GFP (5×10^6 GFP-CIU/head) or SeV/PLmutΔMΔFΔHN-GFP (5×10^6 GFP-CIU/head) was injected into the ear auricle intradermally ($n = 3$). GFP expression was assessed by examining the ear auricle under a fluorescence stereomicroscope. The surface of the auricle was photographed and the GFP intensity was quantified with NIH image software. Sera of injected mice were collected at weekly intervals and stored at − 80 °C until the measurement of neutralizing and total anti-SeV antibody levels.

Immunohistochemical staining

The auricle was frozen and sliced into 10 μm thick sections with a cryotome (Coldtome CM-502; Sakura Seiki). The frozen sections were pretreated with 0.3% H_2O_2 in methanol. Migrated macrophages and pan-T cells were detected using a rabbit polyclonal anti-CD11b (Santa Cruz) and anti-CD3 (Santa Cruz) antibodies, respectively, followed by using a Histofine SAB-PO(R) kit (Nichirei). Immunopositive cells were visualised with 3, 3′-diaminobenzidine tetrahydrochloride (DAB) and counterstained with hematoxylin.

Ex vivo transduction using the M-, F- and HN-genes-deleted SeV vector

MC57G cells, an isogenic cell line of C57BL/6, were inoculated with SeV/ΔF-GFP or SeV/PLmutΔMΔFΔHN-GFP at an MOI of 3. Two days later, the cells were transplanted subcutaneously in the back of C57BL/6 mice. Sera of transplanted mice were collected at weekly intervals.

Quantitation of neutralizing and total anti-SeV antibodies

To quantify neutralizing antibody against SeV, serial 1 : 5 dilutions of sera previously inactivated at 56 °C for 30 min were mixed with wild-type SeV carrying the GFP gene (SeV^{18+}GFP (wild)) at 37 °C for 1 h. These virus-serum mixtures were inoculated to LLC-MK_2 cells in 96-well plates and cultured in serum-free MEM at 37 °C for 3 days. The remaining infectivity of SeV^{18+}GFP (wild) was estimated by measuring the fluorescence of GFP with a fluorescence microplate reader (Cytofluor II; Biosearch/Millipore). Results are expressed as percent inhibition by setting the values from the cells infected with SeV^{18+}GFP (wild) alone as 0% and those from the uninfected cells as 100%. Total anti-SeV antibody level in the sera was subsequently measured by a test kit for HVJ (Denka Seiken) according to the manufacturer's protocol. In this test, the quantities of anti-SeV antibody were measured as relative ones represented by OD450 because the absolute quantity of anti-SeV antibody could not be determined. Those were determined using 1 : 300 dilutions of the sera and measured simultaneously.

Characterization of serum antibodies by Western blotting

The mixture of NP and HN viral proteins which was prepared from infected cells and whole virion proteins were separated by SDS-PAGE and transferred

DOI: 10.1002/jgm

to Immobilon-PVDF membranes (Millipore) as described before. Sera collected from transplanted mice were used as the first antibody. Secondary antibodies were goat anti-mouse IgG+IgM conjugated with horseradish peroxidase.

Results and discussion

Establishment of M-, F- and HN-expressing packaging cell line

For the recovery of SeV/ΔMΔFΔHN virion particles from cDNA, the missing M, F and HN genes must be complemented *in trans*. To establish such an M-, F- and HN-expressing packaging cell line, a Cre/*lox*P induction system [22] was employed as has been reported [15,16]. Moreover, we previously established an M/F-expressing packaging cell line (LLC-MK_2/F7/M#33), in which M- and F-genes-deleted SeV (SeV/ΔMΔF) was successfully recovered [17]. Therefore, it was thought that the introduction of the HN gene into LLC-MK_2/F7/M#33 would make this cell line capable of supporting the recovery of SeV/ΔMΔFΔHN. Early-passage LLC-MK_2/F7/M#33 cells were transfected with pCALNdLw/HN. After incubation at 37 °C for 2 weeks, clones were selected and expanded. The HN protein expression was examined by the Western blot analysis of the cellular proteins after infection with the Cre-encoding adenovirus vector, AxCANCre [21], at a MOI of 5. The clones expressing the HN protein were then subjected to two rounds of subcloning, resulting in the final selection of one cell line, LLC-MK_2/F7/M#33/A/HN7.

Construction of a vector with M, F and HN gene deletions

SeV genomic cDNA carrying the GFP gene in place of the M, F and HN genes (SeV/ΔMΔFΔHN-GFP) was constructed (Figure 1A). The GFP gene in SeV cDNA allows us to confirm easily the successful recovery of the SeV/ΔMΔFΔHN vector. Using the established cell line and the plasmid-based reverse genetics technology [26], we propagated SeV/ΔMΔFΔHN-GFP, leading to a titer of 1×10^8 CIU/ml in the culture supernatant. During the reconstitution of SeV/ΔMΔFΔHN-GFP, some degree of cytotoxicity toward the packaging cell lines, which had not been observed with previous SeV vector reconstitutions, was observed (data not shown). The cause of this cytotoxicity is still obscure, but one possibility is that the L protein might be expressed in relative excess and drive the transcription and replication of the vector beyond the capacity of the packaging cells because of the shorter genome size of SeV/ΔMΔFΔHN-GFP. Based on this hypothesis, we prepared the SeV/PLmutΔMΔFΔHN-GFP vector, which has amino acid substitutions in P (L511F) and L (N1197S, K1795E). These substitutions had been identified in SeV strains capable of persistent infection *in vitro* with slightly reduced transcription and replication [27]. As expected, SeV/PLmutΔMΔFΔHN-GFP was propagated without obvious cytotoxicity during reconstitution, leading to a titer of 5×10^8 CIU/ml in the culture supernatant.

Gene structure of the recovered SeV vector

The vector gene structure was confirmed by RT-PCR. The DNA fragment of SeV/ΔMΔFΔHN-GFP from the 5′-terminus of the P gene to the 3′-terminus of the L gene containing the GFP gene was amplified from the vector genome, and the amplified fragment was compared with the corresponding fragments amplified

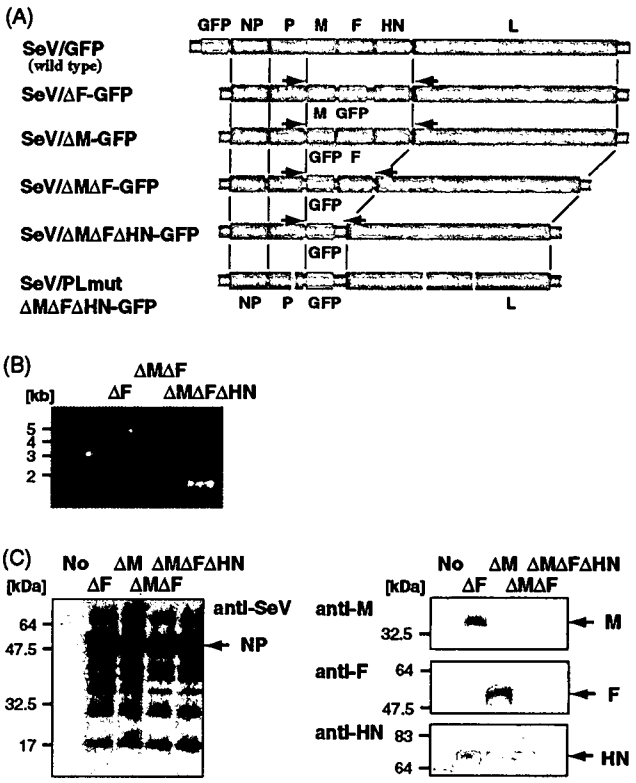

Figure 1. Construction of M-, F- and HN-genes-deleted SeV vector carrying the GFP gene, and confirmation of its structure. (A) The structures of recombinant SeV genomes. The open reading frame of the GFP gene was inserted with the SeV end and start signals (EIS) in the respective positions of the deleted gene(s). The positions of the primers for RT-PCR are shown by arrows. (B) Viral genome structure was confirmed by RT-PCR. The DNA fragment of SeV/ΔMΔFΔHN-GFP (ΔMΔFΔHN) from the 5′-terminal of the P gene to the 3′-terminal of the L gene (containing the GFP gene) was amplified from the vector genome, and the fragment was compared to the corresponding fragments amplified from the vector genomes of SeV/ΔF-GFP (ΔF) and SeV/ΔMΔF-GFP (ΔMΔF). (C) Viral proteins were detected by Western blot analysis. LLC-MK_2 cells were infected with SeV^{18+}GFP (wild), SeV/ΔF-GFP (ΔF), SeV/ΔM-GFP (ΔM), SeV/ΔMΔF-GFP (ΔMΔF) or SeV/ΔMΔFΔHN-GFP (ΔMΔFΔHN) at an MOI of 3. The viral proteins in the cells 2 days after transduction were detected by Western blotting using anti-M, anti-F, anti-HN and anti-SeV (which mainly detects NP protein) antibodies after transferring the proteins to a PVDF membrane

DOI: 10.1002/jgm

from the vector genomes of SeV/ΔF-GFP and SeV/ΔMΔF-GFP. Amplification of 1719-bp, 3576-bp and 4773-bp DNAs for SeV/ΔMΔFΔHN-GFP, SeV/ΔMΔF-GFP and SeV/ΔF-GFP, respectively, was expected based on the genome structures. The results of RT-PCR clearly showed that SeV/ΔMΔFΔHN-GFP had the M, F and HN genes deleted from its genome (Figure 1B). In the case of SeV/PLmutΔMΔFΔHN-GFP, the deletion of the M, F and HN genes was examined by RT-PCR as in the case of SeV/ΔMΔFΔHN-GFP, and newly introduced mutations in the P and L parts were also confirmed by determining the sequences of the DNA fragment amplified from the cDNA (data not shown). The absence of the M, F and HN genes was also confirmed by Western blot analysis of the protein expression of LLC-MK_2 cells infected at an MOI of 3 with SeV/ΔF-GFP, SeV/ΔM-GFP, SeV/ΔMΔF-GFP or SeV/ΔMΔFΔHN-GFP. In these analyses, anti-M, anti-F, anti-HN or anti-SeV (which mainly detects the NP protein) antibodies were used. The NP protein, but not M, F or HN proteins, was detected in the cells transduced with SeV/ΔMΔFΔHN-GFP (Figure 1C). Similarly, neither the M nor the F protein was observed in cells transduced with SeV/ΔMΔF-GFP. These results clearly indicated the absence of the envelope genes in these vectors.

Cytopathic effect of SeV is efficiently diminished by M, F and HN gene deletion

Infection with SeV vectors causes a cytopathic effect (CPE) in some types of cells. Therefore, it was important to characterise the newly recovered SeV/ΔMΔFΔHN-GFP and SeV/PLmutΔMΔFΔHN-GFP in terms of CPE. The CPE was investigated in CV-1 cells, which are known to be very sensitive to SeV infection-dependent cytotoxicity [17]. CV-1 cells plated in 96-well plates were transduced with SeV/ΔF-GFP, SeV/ΔM-GFP, SeV/ΔMΔF-GFP, SeV/ΔMΔFΔHN-GFP and SeV/PLmutΔMΔFΔHN-GFP, respectively, and incubated in serum-free MEM for 3 days. Then, their CPE was quantitatively measured by using Decker's method [25]. The CPE of SeV/ΔMΔFΔHN-GFP was approximately equal to that of SeV/ΔMΔF-GFP. However, that of SeV/PLmutΔMΔFΔHN-GFP was greatly reduced as compared to that of all other types of SeV vectors (Figure 2A). Morphological damage to the cells infected with vectors at an MOI of 20 was also examined under a fluorescence microscope. CV-1 cells transduced with SeV/PLmutΔMΔFΔHN-GFP showed little CPE (Figure 2B). Thus, the combination of the deletion of all envelope-related genes and the amino acid substitutions in P and L was found to be quite effective in reducing the CPE of SeV *in vitro*. In addition to membrane fusion and apoptosis, rapid transcription and replication increase SeV-induced cytotoxicity. The substitutions in P and L that induce slightly reduced transcription and replication [27] brought about additional reduction of CPE.

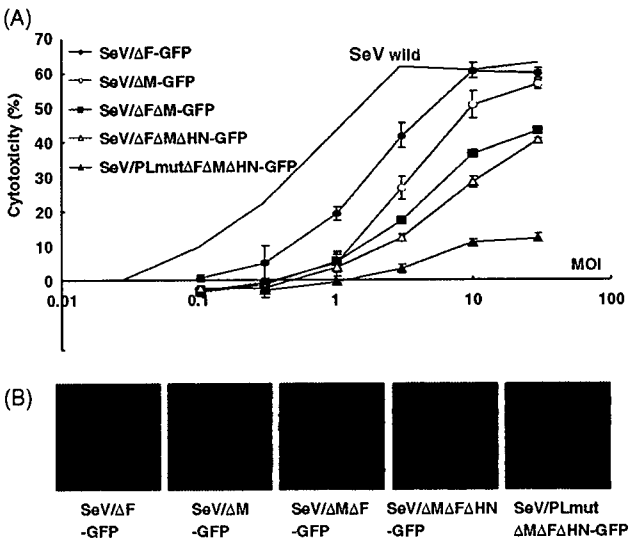

Figure 2. Analysis of SeV infection-dependent cytotoxicity. (A) Quantitative measurement using SeV infection-sensitive cells. CV-1 cells were infected with SeV/ΔF-GFP, SeV/ΔM-GFP, SeV/ΔMΔF-GFP, SeV/ΔMΔFΔHN-GFP or SeV/PLmutΔMΔF-ΔHN-GFP at an indicated MOI. Cytotoxicity was determined by the quantity of LDH released from damaged cells. The assay was carried out 3 days after infection using the supernatants of cultures in serum-free medium. The percentage of cytotoxicity (%) was calculated using the low control (0%) from the supernatant of uninfected cells and the high control (100%) from the supernatant of cell lysates after treatment with 2% Triton X-100. Cytopathic effect of a wild-type SeV (SeV^{18+}GFP (wild)) was also examined and shown in the thin line. (B) Morphology of CV-1 cells infected with respective SeV vectors at an MOI of 20 on day 3 after infection

Quantitative analysis of foreign gene expression of M-, F- and HN-genes-deleted SeV

To quantify the expression level of a foreign gene(s) carried in SeV/ΔMΔFΔHN, the gene for the secreted form of human placental alkaline phosphatase (SEAP), which is an easily detectable marker of protein production, was inserted upstream of the open reading frame of NP. The thus-generated SeV^{18+}SEAP/PLmutΔMΔFΔHN-GFP vector was used for the SEAP assay. LLC-MK_2 cells were infected at an MOI of 3 with SeV^{18+}SEAP/ΔF-GFP, SeV^{18+}SEAP/ΔMΔF-GFP [17] or SeV^{18+}SEAP/PLmutΔ-MΔFΔHN-GFP and the culture supernatants were collected every 24 h. The expression level of SEAP in the culture supernatant of SeV^{18+}SEAP/PLmutΔMΔFΔHN-GFP was rather low as compared to that of SeV^{18+}SEAP/ΔF-GFP, but was similar to that of SeV^{18+}SEAP/ΔMΔF-GFP (Figure 3). This supported the notion that the M protein might participate not only in viral assembly and budding, but also in the control of transgene transcription [28].

Prolonged transgene expression of M-, F- and HN-genes-deleted SeV *in vivo*

We next examined the transduction efficiency of SeV/PLmutΔMΔFΔHN-GFP *in vivo*. SeV/PLmutΔMΔF-

DOI: 10.1002/jgm

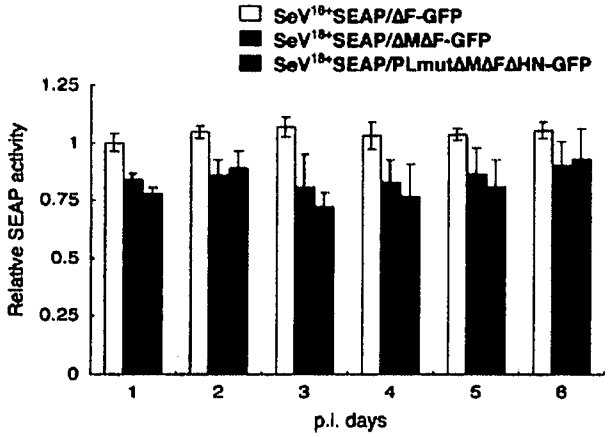

Figure 3. Comparison of expression performance of SeV vectors carrying the SEAP gene. The culture medium of LLC-MK_2 cells was collected every 24 h after infection with SeV^{18+}SEAP/ΔF-GFP, SeV^{18+}SEAP/ΔMΔF-GFP or SeV^{18+}SEAP/ΔMΔFΔHN-GFP at an MOI of 3. SEAP activity was determined as a relative activity by setting the value from the medium of uninfected cells as zero (0) and that from the medium of SeV^{18+}SEAP/ΔF-GFP-infected cells (MOI = 3, 1 day post-infection.) as one (1). Average of three experiments; bar: SD

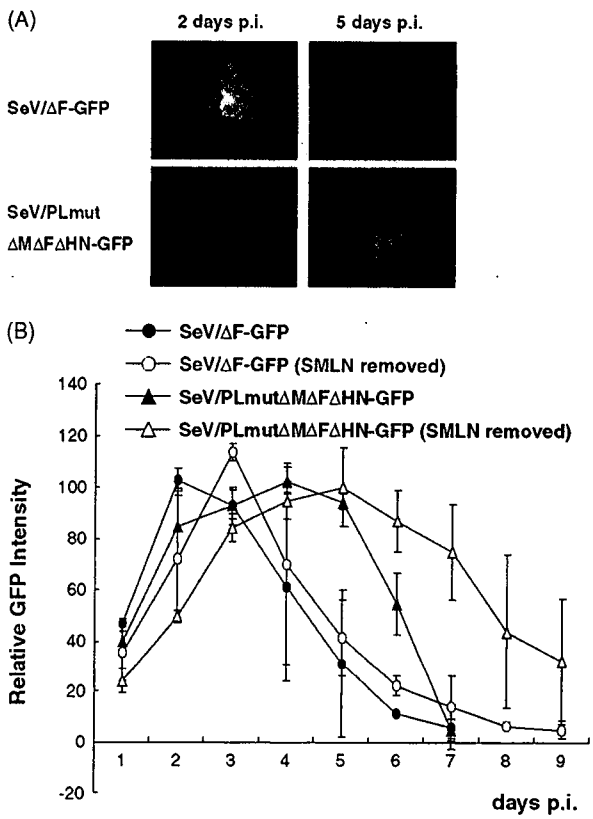

Figure 4. Gene transfer by M-, F- and HN-genes-deleted SeV vector *in vivo*. (A) Gene transfer to the ear auricle. SeV/ΔF-GFP or SeV/PLmutΔMΔFΔHN-GFP (5×10^6 GFP-CIU/head) was administered to the ear auricle of BALB/cA mice with or without submandibular lymph nodes (SMLN) by a single intradermal injection (n = 3). GFP expression was detected by a fluorescent stereomicroscope from the skin surface of the ear auricle under a fixed condition. (B) Quantitative analysis of GFP fluorescence. The expression of GFP was calculated by multiplying its fluorescence intensity and its area by NIH image software and expressed as relative ones

ΔHN-GFP or SeV/ΔF-GFP was administered intradermally to the ear auricles of BALB/cA mice (5×10^6 CIU/head). We can directly observe the fluorescence from expressed GFP over a period of time through the skin surface of the ear auricle without sacrificing animals. Efficient transduction from both vectors was confirmed and the level of GFP expression was approximately equal between SeV/ΔF-GFP and SeV/PLmutΔMΔFΔHN-GFP (Figure 4A). However, the peak of expression was prolonged in the case of SeV/PLmutΔMΔFΔHN-GFP (Figure 4B). In an additional study, SeV vectors were administered after the removal of submandibular lymph nodes in order to avoid direct transduction to them. In this case, GFP expression derived from SeV/PLmutΔMΔFΔHN-GFP was significantly prolonged (Figure 4B). In fact, both anti-CD11b (macrophage marker) and anti-CD3 (Pan-T cell marker) staining of the frozen sections of the inoculated auricles showed the delayed migration of macrophages and T cells to the site of SeV/PLmutΔMΔFΔHN-GFP administration compared with that of SeV/ΔF-GFP (Figures 5A and 5B). These results clearly indicate that the immunoreaction against SeV/PLmutΔMΔFΔHN-GFP is weak and delayed compared to that against SeV/ΔF-GFP. Efficient transduction and prolonged expression of SeV/PLmutΔMΔFΔHN were also observed in the cases of transduction to the airway epithelial cells and neuronal cells in the brain (data not shown).

Humoral immune reaction of M-, F- and HN-genes-deleted SeV *in vivo*

We next examined the effect of SeV/PLmutΔMΔFΔHN-GFP on the induction of anti-SeV antibodies and neutralizing antibodies. SeV/PLmutΔMΔFΔHN-GFP or SeV/ΔF-GFP was administered to BALB/cA mice, and sera of mice were collected weekly for 3 weeks. Phosphate-buffered saline (PBS)-injected mice were used as controls. The level of serum neutralizing antibodies in the mice administered SeV/PLmutΔMΔFΔHN-GFP was reduced to about half of that in the mice administered SeV/ΔF-GFP (Figure 5C). On the other hand, the overall quantity of anti-SeV antibodies was only slightly reduced by using the new SeV vector. The envelope proteins of SeV/PLmutΔMΔFΔHN-GFP particles supplied by the packaging cells may contribute to the induction of both overall anti-SeV antibodies and a certain amount of neutralizing antibodies against the vector.

No neutralizing antibody production after M-, F- and HN-genes-deleted SeV transduction *ex vivo*

We then examined whether the envelope gene deletions reduce the induction of humoral immunoreaction

DOI: 10.1002/jgm

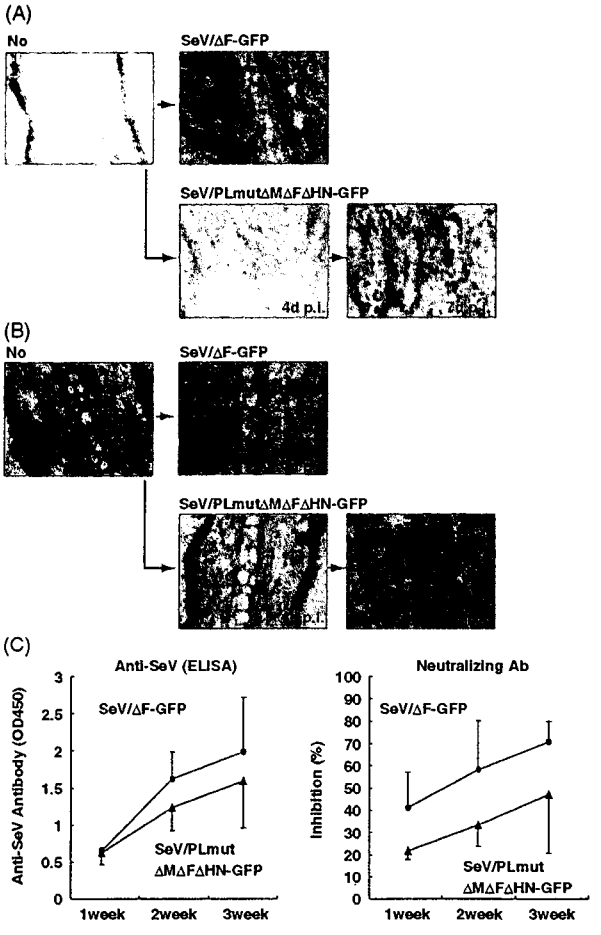

Figure 5. Immune reaction to SeV vectors introduced by *in vivo* transduction. Immunohistochemical analysis of the migrations of (A) macrophages and (B) T lymphocytes. The frozen sections of ear auricles of BALB/cA mice intradermally administered with SeV/ΔF or SeV/PLmutΔMΔFΔHN. (C) Sera from mice administered with SeV/ΔF-GFP or SeV/PLmutΔMΔFΔHN-GFP were assayed for overall anti-SeV antibodies as well as neutralizing antibodies directed against SeV. Neutralizing antibody level is shown as a percent inhibition of $SeV^{18+}GFP$ (wild) infectivity

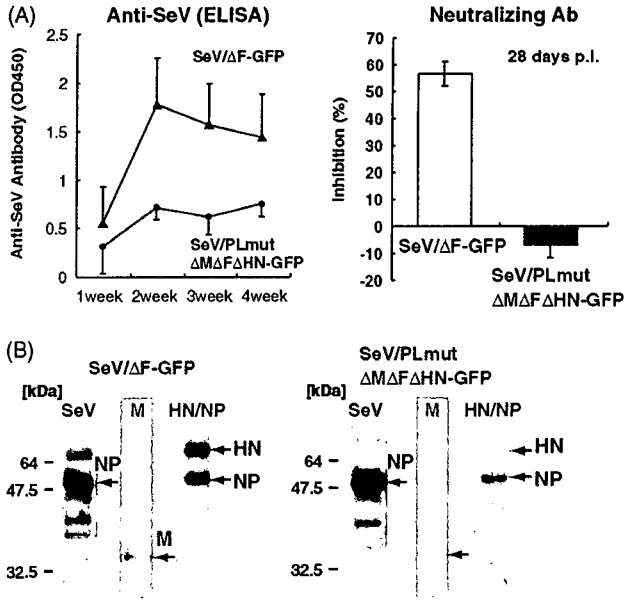

Figure 6. Immune reaction to SeV vectors following transplantation of SeV-infected cells. (A) Serum levels of anti-SeV antibody (left) following transplantation of isogenic cells (1×10^6 cells/head) infected with SeV/ΔF-GFP or SeV/PLmutΔMΔFΔHN-GFP at an MOI of 3 were examined. Neutralizing antibody level was measured in the sera on days 28 after transplantation (right). (B) Serum was analysed by Western blotting. The purified M protein, the mixture of NP and HN viral proteins that were prepared from infected cells, and whole virion proteins were loaded and transferred to a membrane. Western blotting was carried out using sera collected from mice transplanted with isogenic cells infected with SeV vectors as a primary antibody

in the case of *ex vivo* transduction. Isogenic cells (MC57G; 1×10^6 cells) transduced by SeV/PLmutΔMΔFΔHN-GFP or SeV/ΔF-GFP were transplanted subcutaneously in the backs of C57BL/6 mice. Sera were collected at weekly intervals, and the levels of anti-SeV and SeV-neutralizing antibodies were measured. Figure 6A shows that, in comparison with the overall quantity of anti-SeV antibody produced in the case of transduction with SeV/ΔF-GFP, the production of anti-SeV antibody was greatly reduced when SeV/PLmutΔMΔFΔHN-GFP was used. Furthermore, neutralizing antibody was undetectable in mice transplanted with cells transduced by SeV/PLmutΔMΔFΔHN-GFP even at 28 days after the transplantation. The serum antibodies were characterised by Western blot analysis. Anti-HN and anti-M antibodies were not detected in the serum from the mice transplanted with SeV/PLmutΔMΔFΔHN-GFP-transduced cells (Figure 6B). However, anti-NP antibody was detected in mice transplanted with either SeV/ΔF-GFP- or SeV/PLmutΔMΔFΔHN-GFP-transduced cells. As the HN protein is known to be one of the major targets for neutralizing antibodies against SeV [29], the abolishment of neutralizing antibody in the case of SeV/PLmutΔMΔFΔHN-GFP would be caused by the absence of anti-HN antibody in the serum. Also, we previously showed that deletion of both the M and F genes from the vector genome made the SeV vector non-transmissible and caused a lack of the formation of particles that might have enhanced the immunogenicity [12]. These results clearly indicate that the deletion of all three envelope-related genes (M, F and HN) from the SeV genome significantly reduced the humoral immune reaction against the SeV vector, especially in *ex vivo* transduction.

In conclusion, we have successfully recovered and propagated a high titer of more than 10^8 CIU/ml of a new SeV vector (SeV/ΔMΔFΔHN), in which all envelope-related genes were deleted from the vector genome using a newly established packaging cell line. Amino acid substitutions in P and L proteins that induce a slower rate of transcription caused additional attenuation of this vector (SeV/PLmutΔMΔFΔHN). This new vector showed efficient transduction capability both *in vitro* and *in vivo*. Furthermore, *in vivo* as well as *ex vivo* experiments showed a significant reduction of its immunogenicity compared with that of SeV/ΔF. That is, the deletion of

DOI: 10.1002/jgm

gene(s) from the SeV genome and additional introduction of amino acid substitutions into P and L is a very effective way to reduce both the immunogenic and cytopathic reactions induced by the SeV vector. These modifications are expected to improve the safety and broaden the range of clinical applications of SeV vectors such as for vaccine treatments [8,9] and cell-based treatment for hematopoietic damage including repeated dosing. The new vector, SeV/PLmutΔMΔFΔHN, is one of the most advanced genotoxicity-free cytoplasmic RNA virus vectors. This vector will also become a possible source for further improvement of SeV vector systems by introducing the additional mutations on the NP gene to modify the immune response against the vector and for alternative vector candidates such as virus-like particles (VLPs) and self-replicating ribonucleoprotein (RNP) complexes [3].

Acknowledgements

We acknowledge I. Saito for supplying AxCANCre; H. Iba for supplying pCALNdLw; H. Taira for supplying anti-F and anti-HN antibodies; K. Washizawa, S. Fujikawa, T. Kanaya, T. Yamamoto, and A. Tagawa for excellent technical assistance; and A. Kato, Y. F. Zhu, H. Hara, and Y. Ueda for helpful discussions.

References

1. Lamb RA, Kolakofsky D. *Paramyxoviridae*: the viruses and their replication. In *Fields Virology*, Fields BN, Knipe DM, Howley PM (eds). Lippincott-Raven: Philadelphia, 1996; 1177–1204.
2. Bitzer M, Armeanu S, Lauer UM, *et al.* Sendai virus vectors as an emerging negative-strand RNA viral vector system. *J Gene Med* 2003; 5: 543–553.
3. Griesenbach U, Inoue M, Hasegawa M, *et al.* Sendai virus for gene therapy and vaccination. *Curr Opin Mol Ther* 2005; 7: 346–352.
4. Masaki I, Yonemitsu Y, Yamashita A, *et al.* Angiogenic gene therapy for experimental critical limb ischemia: acceleration of limb loss by overexpression of vascular endothelial growth factor 165 but not of fibroblast growth factor-2. *Circ Res* 2002; 90: 966–973.
5. Shoji T, Yonemitsu Y, Komori K, *et al.* Intramuscular gene transfer of FGF-2 attenuates endothelial dysfunction and inhibits intimal hyperplasia of vein grafts in poor-runoff limbs of rabbit. *Am J Physiol Heart Circ Physiol* 2003; 285: H173–182.
6. Iwadate Y, Inoue M, Saegusa T, *et al.* Recombinant Sendai virus vector induces complete remission of established brain tumors through efficient interleukin-2 gene transfer in vaccinated rats. *Clin Cancer Res* 2005; 11: 3821–3827.
7. Kinoh H, Inoue M, Washizawa K, *et al.* Generation of a recombinant Sendai virus that is selectively activated and lyses human tumor cells expressing matrix metalloproteinases. *Gene Ther* 2004; 11: 1137–1145.
8. Matano T, Kobayashi M, Igarashi H, *et al.* Cytotoxic T lymphocyte-based control of simian immunodeficiency virus replication in a preclinical AIDS vaccine trial. *J Exp Med* 2004; 199: 1709–1718.
9. Takeda A, Igarashi H, Nakamura H, *et al.* Protective efficacy of an AIDS vaccine, a single DNA priming followed by a single booster with a recombinant replication-defective Sendai virus vector, in a macaque AIDS model. *J Virol* 2003; 77: 9710–9715.
10. Morrison T, McQuain C, McGinnes L. Complementation between avirulent Newcastle disease virus and a fusion protein gene expressed from a retrovirus vector: requirements for membrane fusion. *J Virol* 1991; 65: 813–822.
11. Arnon TI, Lev M, Katz G, *et al.* Recognition of viral hemagglutinins by NKp44 but not by NKp30. *Eur J Immunol* 2001; 31: 2680–2689.
12. Guertin DP, Fan DP. Stimulation of cytolytic T cells by isolated viral peptides and HN protein coupled to agarose beads. *Nature* 1980; 283: 308–311.
13. Justice PA, Sun W, Li Y, *et al.* Membrane vesiculation function and exocytosis of wild-type and mutant matrix proteins of vesicular stomatitis virus. *J Virol* 1995; 69: 3156–3160.
14. Mebatsion T, Konig M, Conzelmann KK. Budding of rabies virus particles in the absence of the spike glycoprotein. *Cell* 1996; 84: 941–951.
15. Li H-O, Zhu YF, Asakawa M, *et al.* A cytoplasmic RNA vector derived from nontransmissible Sendai virus with efficient gene transfer and expression. *J Virol* 2000; 74: 6564–6569.
16. Inoue M, Tokusumi Y, Ban H, *et al.* A new Sendai virus vector deficient in the matrix gene does not form virus particles and shows extensive cell-to-cell spreading. *J Virol* 2003; 77: 6419–6429.
17. Inoue M, Tokusumi Y, Ban H, *et al.* Recombinant Sendai virus vectors deleted in both the matrix and the fusion genes: efficient gene transfer with preferable properties. *J Gene Med* 2004; 6: 1069–1081.
18. Inoue M, Tokusumi Y, Ban H, *et al.* Nontransmissible virus-like particle formation by F-deficient Sendai virus is temperature sensitive and reduced by mutations in M and HN proteins. *J Virol* 2003; 77: 3238–3246.
19. Bernloehr C, Bossow S, Ungerechts G, *et al.* Efficient propagation of single gene deleted recombinant Sendai virus vectors. *Virus Res* 2004; 99: 193–197.
20. Hamaguchi M, Yoshida T, Nishikawa K, *et al.* Transcriptive complex of Newcastle disease virus. I. Both L and P proteins are required to constitute an active complex. *Virology* 1983; 128: 105–117.
21. Kanegae Y, Takamori K, Sato Y, *et al.* Efficient gene activation system on mammalian cell chromosomes using recombinant adenovirus producing Cre recombinase. *Gene* 1996; 181: 207–212.
22. Arai T, Matsumoto K, Saitoh K, *et al.* A new system for stringent, high-titer vesicular stomatitis virus G protein-pseudotyped retrovirus vector induction by introduction of Cre recombinase into stable prepackaging cell lines. *J Virol* 1998; 72: 1115–1121.
23. Segawa H, Kato M, Yamashita T, *et al.* The roles of individual cysteine residues of Sendai virus fusion protein in intracellular transport. *J Biochem (Tokyo)* 1998; 123: 1064–1072.
24. Miura N, Uchida T, Okada Y. HVJ (Sendai virus)-induced envelope fusion and cell fusion are blocked by monoclonal anti-HN protein antibody that does not inhibit hemagglutination activity of HVJ. *Exp Cell Res* 1982; 141: 409–420.
25. Decker T, Lohmann-Matthes ML. A quick and simple method for the quantitation of lactate dehydrogenase release in measurements of cellular cytotoxicity and tumor necrosis factor (TNF) activity. *J Immunol Methods* 1988; 115: 61–69.
26. Kato A, Sakai Y, Shioda T, *et al.* Initiation of Sendai virus multiplication from transfected cDNA or RNA with negative or positive sense. *Genes Cells* 1996; 1: 569–579.
27. Bossow S, Neubert WJ. A set of four mutations in the P and L genes derived from persistent Sendai virus variants attenuates viral replication. *Negative Strand Viruses* 2000; 157.
28. Ogino T, Iwama M, Ohsawa Y, *et al.* Interaction of cellular tubulin with Sendai virus M protein regulates transcription of viral genome. *Biochem Biophys Res Commun* 2003; 311: 283–293.
29. Tozawa H, Komatsu H, Ohkata K, *et al.* Neutralizing activity of the antibodies against two kinds of envelope glycoproteins of Sendai virus. *Arch Virol* 1986; 91: 145–161.

Induction of Efficient Antitumor Immunity Using Dendritic Cells Activated by Recombinant Sendai Virus and Its Modulation by Exogenous *IFN-β* Gene[1]

Satoko Shibata,*† Shinji Okano,* Yoshikazu Yonemitsu,[2]* Mitsuho Onimaru,* Shihoko Sata,* Hiroko Nagata-Takeshita,* Makoto Inoue,‡ Tsugumine Zhu,‡ Mamoru Hasegawa,‡ Yoichi Moroi,† Masutaka Furue,† and Katsuo Sueishi*

Dendritic cell (DC)-based cancer immunotherapy has been paid much attention as a new and cancer cell-specific therapeutic in the last decade; however, little clinical outcome has been reported. Current limitations of DC-based cancer immunotherapy include sparse information about which DC phenotype should be administered. We here report a unique, representative, and powerful method to activate DCs, namely recombinant Sendai virus-modified DCs (SeV/DC), for cancer immunotherapy. In vitro treatment of SeV without any bioactive gene solely led DCs to a mature phenotype. Even though the expression of surface markers for DC activation ex vivo did not always reach the level attained by an optimized amount of LPS, superior antitumor effects to B16F1 melanoma, namely tumor elimination and survival, were obtained with use of SeV-GFP/DC as compared with those seen with LPS/DC in vivo, and the effect was enhanced by SeV/DC-expressing IFN-β (SeV-murine IFN-β (mIFN-β)/DC). In case of the treatment of an established tumor of B16F10 (7–9 mm in diameter), a highly malignant subline of B16 melanoma, SeV-modified DCs (both SeV-GFP/DC and SeV-mIFN-β/DC), but not immature DC and LPS/DC, dramatically improved the survival of animals. Furthermore, SeV-mIFN-β/DC but not other DCs could lead B16F10 tumor to the dormancy, associated with strongly enhanced $CD8^+$ CTL responses. These results indicate that rSeV is a new and powerful tool as an immune booster for DC-based cancer immunotherapy that can be significantly modified by IFN-β, and SeV/DC, therefore, warrants further investigation as a promising alternative for cancer immunotherapy. *The Journal of Immunology,* **2006, 177: 3564–3576.**

Cancer vaccines have focused on the induction of CTLs that specifically attack tumor cells in an Ag-restricted manner without exerting a significantly harmful effect on nontumor cells. The induction of tumor-specific $CD4^+$ T cells is also important not only in helping the $CD8^+$ CTL response but also in mediating antitumor effector functions through the induction of eosinophils and macrophages (1). To boost these immune responses, several substances have been used as cancer vaccines, including gene-modified autologous tumor cells, peptide vaccine, plasmid DNA, and Ag-loaded dendritic cells (DCs)[3] (2). Despite current extensive efforts by physicians and scientists in clinical studies of cancer immunotherapy, very little clinical outcome has been reported (3).

DCs are the most potent and professional APCs that determine either Th1 or Th2 polarization of naive T cells, and they have been a promising tool for cancer immunotherapy. The immature state of DCs is known to be appropriate for Ag processing, and in turn, they must be matured to fully activated DCs, which express high levels of cell surface MHC-Ag complex and costimulatory molecules, for a sufficiently productive CTL response (4). Since the first promising clinical study of a DC-based cancer vaccine was reported in 1996 (5), similar studies have been performed using this type of vaccine against several cancers, including metastatic melanoma, all over the world (6–7). These early clinical trials suggested the potential of DC-based immunotherapy, but the extensive follow-up studies concluded that the current strategy remains immature as a standard therapeutic for cancer treatment (2).

Current issues of DC-based cancer immunotherapy include a lack of information regarding the following points: 1) the most effective DC subtypes, 2) the optimal conditions and activation stimuli to generate activated DCs showing optimal antitumor effect in vivo, 3) the optimal route for administration, and 4) the optimal dose and frequency of DC vaccinations (2). Because no one knows what the optimal performance and precise clinical indications of DC-based cancer immunotherapy are at present, preclinical assessment regarding these points in detail is absolutely required to obtain more data about DC therapy in clinical settings.

Currently, "virotherapy" is an indicative term for tumor-selective oncolytic virus therapy for cancer, namely "oncolytic virotherapy" (8). However, the first use of the term virotherapy appeared in a Japanese article in 1960, demonstrating the modest antitumor effect of a direct intratumor (i.t.) and/or intradermal injection of bovine vaccinia virus for patients with skin cancers (9).

*Division of Pathophysiological and Experimental Pathology, Department of Pathology and †Department of Dermatology, Graduate School of Medical Sciences, Kyushu University, Fukuoka, Japan; and ‡DNAVEC Corporation, Tsukuba, Ibaraki, Japan

Received for publication August 11, 2005. Accepted for publication June 23, 2006.

The costs of publication of this article were defrayed in part by the payment of page charges. This article must therefore be hereby marked *advertisement* in accordance with 18 U.S.C. Section 1734 solely to indicate this fact.

[1] This work was supported in part by a Grant-in-Aid (to Y.Y. and K.S.) from the Japanese Ministry of Education, Culture, Sports, Science, and Technology; and by the Program for Promotion of Fundamental Studies in Health Sciences of the National Institute of Biomedical Innovation (to Y.Y. and K.S.; Project MF-21).

[2] Address correspondence and reprint requests to Dr. Yoshikazu Yonemitsu, Division of Pathophysiological and Experimental Pathology, Department of Pathology, Graduate School of Medical Sciences, Kyushu University, 3-1-1 Maidashi, Higashi-ku, Fukuoka 812-8582, Japan. E-mail address: yonemitu@med.kyushu-u.ac.jp

[3] Abbreviations used in this paper: DC, dendritic cell; SeV, recombinant Sendai virus; SeV/DC, SeV-modified DC; mIFN-β, murine IFN-β; mBM-DC, bone marrow-derived DC; i.t., intratumoral; T-reg, regulatory T; MOI, multiplicity of infection; LCMV, lymphocytic choriomeningitis virus; fsc/ssc, forward scatter/side scatter.

0022-1767/06/$02.00

This use of the term virotherapy, therefore, included the concept of "immunostimulatory virotherapy."

In the last decade, we extensively examined the use of recombinant Sendai virus (SeV) as a novel and powerful gene transfer agent as the cytoplasmic gene expression system (10–12). SeV, a member of family *Paramyxoviridae*, has a nonsegmented negative-strand RNA genome and makes use of sialic acid residue on surface glycoprotein or asialoglycoprotein present on most cell types as a receptor (13, 14). As SeV uses a cytoplasmic transcription system, it can mediate gene transfer to a cytoplasmic location, avoiding possible malignant transformation due to genetic alteration of host cells (10, 15), that is a safety advantage of SeV. Furthermore, there are technical advantages in the use of rSeV as a gene therapy vector; first, the infectious activity of SeV particles is stable to be easily concentrated to high titers by ultracentrifugation, which is in clear contrast to the features of retroviral vectors. Second, and most importantly, the modalities of target cell processing and viral transduction are technically nondemanding and feasible in clinical situations that require transduction into large numbers of target cells, including hemopoietic stem cells (16). Despite these advantageous features of SeV in clinical gene therapy strategies over the other vector systems (10–12), the related immune responses due to virus administration in vivo have been hazardous to expand the use of this mode of vector in the clinical setting, similar to other viral vectors including adenoviruses. During extensive assessment of the mechanisms of immune responses against SeV, we found that ex vivo infection of SeV to immature DCs resulted in their maturation and activation spontaneously, suggesting their possible use for cancer immunotherapy as an immunostimulatory virotherapy.

In the present study, for the first time, we show that i.t. administration of replication-competent SeV-modified DCs (SeV/DCs) induces a dramatically efficient antitumor effect on established tumors in vivo, an effect comparable to that seen with DCs treated with LPS that is well-known as a strong DC stimulator irrelevant to clinical use. Furthermore, we here show that antitumor immunity against an IFN-β-sensitive tumor, a B16 melanoma, is strongly enhanced by the use of SeV/DCs expressing a foreign *IFN-β* gene.

Materials and Methods

Mice and tumor cell lines

Female 6- to 8-wk-old C57BL/6 mice (H-2^b, for B16 melanomas) and C3H/HeN mice (H-2^k, for MH134) of Charles River grade were obtained from KBT Orientals and kept under specific pathogen-free and humane conditions. Murine malignant melanoma B16F1 and B16F10 cells were purchased from American Culture Collections (ATCC). MH134, a murine hepatocellular carcinoma cell line, and X5563, a plasmacytoma cell line derived from C3H/HeN mice, were maintained as described (17). An NK-sensitive lymphoma cell line, YAC-1, and a T cell lymphoma cell line of C57BL/6 mice origin, EL-4, were also purchased from ATCC. These cell lines were maintained in complete medium (RPMI 1640 medium; Sigma-Aldrich) supplemented with 10% FCS (BioWest), penicillin, and streptomycin under a humidified atmosphere containing 5% CO_2 at 37°C.

Recombinant SeVs

rSeVs were constructed as described previously (10). In brief, the entire cDNA-coding jelly fish enhanced GFP (for SeV-GFP), luciferase (for SeV-luciferase), and murine IFN-β (for SeV-mIFN-β) were amplified by PCR, using primers with a *NotI* site and new sets of SeV E and S signal sequence tags for an exogenous gene, and then inserted into the *NotI* site of the cloned genome. Template SeV genomes with an exogenous gene and plasmids encoding N, P, and L proteins (plasmids pGEM-N, pGEM-P, and pGEM-L, respectively) were conjugated with commercially available cationic lipids, then cotransfected with UV-inactivated vaccinia virus vT7–3 into LLMCK2 cells. Forty hours later, the cells were disrupted by three cycles of freezing and thawing and injected into the chorioallantoic cavity of 10-day-old embryonated chicken eggs. Subsequently, the virus was recovered and the vaccinia virus was eliminated by a second propagation in eggs. Virus titer was determined using chicken RBC in a hemagglutination assay, and viruses were kept frozen at −80°C until use. Expression of mIFN-β was confirmed by Western blotting in the culture medium of COS7 cells and DCs transfected with SeV-mIFN-β (data not shown).

Generation of DCs and transfection with SeVs

When preparing murine bone marrow-derived DCs (mBM-DCs), we paid serious attention to maintaining an endotoxin-free condition using endotoxin-free reagents throughout this study. mBM-DCs were generated as previously described with minor modification (18, 19). Briefly, bone marrow cells from C57BL/6 or C3H/HeN mice were collected and passed through a nylon mesh, and RBC and lineage-positive (B220, CD5, CD11b, Gr-1, TER119, 7/4) cells were depleted by using the SpinSep mouse hemopoietic progenitor enrichment kit (StemCell Technologies). These lineage-negative cells (5–10 × 10^4/5 ml/well) were cultured in 50 ng/ml GM-CSF (PeproTech) and 25 ng/ml IL-4 (PeproTech) in endotoxin-free complete medium in 6-well plates. On day 4, half of the culture medium was replaced by fresh medium supplemented with GM-CSF and IL-4 at the same concentration. On day 7, DCs were collected and used for subsequent experiments. For SeV-mediated transduction, DCs (1 × 10^6 cells/ml) were simply incubated with SeVs at an indicated multiplicity of infection (MOI) without any supplementation.

In vitro cytotoxic assay with IFN-β

B16F1, B16F10, and MH134 cells were seeded in 96-well plates at 5000 cells/well, and 24 h later, recombinant murine IFN-β (rmIFN-β; PBL Biomedical Laboratories) was added to each well at various concentrations. Forty-eight hours later, cell viability was assessed by a modified MTT assay using a Cell Counting Kit-8 (Dojin Laboratories). Results were calculated as the percentage of viability = (OD of sample − OD of blank)/(OD of A − OD of blank) × 100, where OD corresponds to A wells without rmIFN-β.

Influence of MHC class I expression on tumor cells by IFN-β

B16F1, B16F10, and MH134 cells (1 × 10^5/ml) were incubated in the presence or absence of rmIFN-β (1000 U/ml) at 37°C for 48 h. B16 or MH134 cells were collected and stained with FITC-conjugated anti-mouse H-$2K^b$ or H-$2K^k$ (BD Pharmingen), respectively, and were analyzed using a FACSCalibur (BD Biosciences). Dead cells were excluded by staining with propidium iodide.

Luciferase assay

The collected mBM-DCs were treated with lysis buffer (Promega) with a protease inhibitor mixture (10), centrifuged, and 20 μl of the supernatant was subjected to luciferase assay. Light intensity was measured after 10 s of preincubation at room temperature using a luminometer (model LB9507; EG&G Berthold) with 10 s integration. Protein concentrations were measured by Bradford's method using a commercially available protein assay system (Bio-Rad) (11). The data were expressed as relative light units per milligram of protein, and each sample was measured more than twice.

Flow cytometric analysis for costimulation-related molecules on DCs

DCs were plated in fresh medium (1 × 10^6 cells/ml) and were incubated with SeV-GFP or SeV-mIFN-β, each at a MOI of 40, or LPS (2 μg/L) for 48 h. Biotinylated anti-mouse I-Ab, CD40, CD80, CD86, CCR7, ICAM-1, and allophycocyanin-conjugated anti-CD11c (BD Pharmingen) mAbs were used for each primary Ab. The collected DCs were centrifuged and incubated with 100 μl of the supernatant from cultured hybridoma-producing anti-mouse CD16/32 mAb (2.4G2; from ATCC) for 30 min at 4°C. The cells were incubated with primary Abs for 30 min at 4°C, and biotinylated Abs were detected by subsequent staining with streptavidin-PE (BD Pharmingen). Just before application to the cytometer, we added 125 ng of propidium iodide to cell suspension to exclude dead cells. Cells were analyzed using a FACSCalibur with the CellQuest software (BD Biosciences Japan). Data analysis was performed using FlowJo 4.5 software (Tree Star).

Cytokine production of cultured DCs

The cultured DCs were plated in fresh medium (1 × 10^6 cells/ml) and were incubated with SeV-GFP or SeV-mIFN-β (MOI of 40) or LPS (2 μg/l) for 48 h. The culture medium were harvested and were measured the concentration of murine IFN-β, IFN-γ, IL-12 p70, TNF-α, and IL-1β by quantitative sandwich enzyme immunosorbent assay using mouse IFN-β, IFN-γ,

IL-12 p70, TNF-α, and IL-1β ELISA kit (R&D Systems) according to the manufacturer's instructions.

DC-based immunotherapy of the established tumor

B16F1 melanoma: early treatment regimen (see Fig. 2). For tumor lysate preparation, B16 melanoma cells were harvested and processed by three rapid cycles of freezing and thawing. As a control, mBM-DCs with neither tumor lysate nor stimulator were used. The other mBM-DCs were pulsed with tumor lysate (ratio of DC number to number of tumor cells for lysate = 1:3) for 18 h and then were incubated with SeV-GFP (MOI = 40; SeV-GFP/DCs), SeV-mIFN-β (MOI = 40; SeV-mIFN-β/DCs), or LPS (2 μg/L; LPS/DCs) for 8 h. Then all DCs were added with 50 μg/ml polymyxin B (Sigma-Aldrich) and were carefully washed two times before injection. Intradermal implantation (C57BL/6 for 1×10^5 B16F1 cells) was done onto the abdomen on day 0, and 1×10^6 DCs were injected i.t. on days 3, 10, and 17. For all injections, materials were suspended in a 100-μl volume of PBS. The size of tumors was assessed using microcalipers three times a week, and the volume was calculated by the following formula: (tumor volume; mm^3) = 0.5236 × (long axis) × (short axis) × (height) (20).

B16F10 melanoma and MH134 hepatocellular carcinoma: later treatment regimen (see Fig. 4). To examine the potentials of cancer vaccines tested here to treat highly malignant phenotypes in vivo, we further assessed "later treatment regimen" when the tumors were well-established and vascularized (7–9 mm in diameter) (3).

DCs were collected as described above, except for control DCs which were pulsed with tumor lysate but not stimulated. Intradermal implantation (C57BL/6 for 1×10^5 B16F10 cells and C3H/HeN for 1×10^6 MH134 cells) was done onto the abdomen on day 0, and 1×10^6 DCs were injected i.t. on days 10, 17, and 24. The size of tumors was assessed as described above.

^{51}Cr release assay for cytolytic activity of NK cells and CTLs

Prepared DCs were i.t. administered three times into tumor-bearing C57BL/6 mice (B16F10) or C3H/HeN mice (MH134) at 1×10^6 cells/100 μl on days 10, 17, and 24. One week after the last immunization, splenocytes were obtained and contaminated erythrocytes were depleted by 0.83% ammonium chloride. For NK cell-lysis assay, the splenocytes were directly used as NK effector cells. For CTL assay, 4×10^6 splenocytes were cultured with 1 μM TRP-2 peptide ($H\text{-}2^b$-restricted peptide = SVYDFFVWL) (21) for B16 melanoma model, or with 3×10^5 inactivated MH134 cells treated with 100 μg/ml mitomycin for the MH134 model in 1 ml of complete medium in a 24-well culture plate. Two days later, 30 IU/ml human rIL-2 was added to the medium. After 5 days, the cultured cells were collected and used as CTL effector cells. Target cells (YAC-1, TRP2-peptide-pulsed EL-4, lymphocytic choriomeningitis virus (LCMV) peptide (H-2b-restricted peptide = AVYNFATCGI) pulsed EL-4 (for third party of B16), MH134 cells, and X5633 (for third party of MH134)) were labeled with 100 μCi $Na_2{}^{51}CrO_4$ for 1.5 h, and Cr release assay was performed as previously described (22). The percentage of specific ^{51}Cr release of triplicates was calculated as follows: ((experimental cpm − spontaneous cpm)/(maximum cpm − spontaneous cpm)) × 100. Spontaneous release was always <10% of maximal Cr release (target cells in 1% Triton X-100).

In vivo depletion of immune cell subsets

Anti-CD4 and anti-CD8 mAbs (250 μg/dose) were derived from GK1.5 and 53-6.72 hybridoma cells, respectively (23, 24). Anti-asialo GM1 (Wako) was given i.p. (50 μg/dose) for NK cell depletion. Elimination of $CD4^+$ or $CD8^+$ cells in tumor-bearing mice (n = 4–5 in each group) was done by i.p. injection of mAbs on days 5, 6, 7, 10, 13, 16, 19, 21, 24, 27, and 30 after the primary tumor inoculation. Flow cytometry confirmed >98% depletion of the target cells for at least 7 days after injection in all animals.

Histopathological analysis

B16F10 tumor was treated twice (days 10 and 17), and freshly excised tumor tissues on day 20 were divided into the longitudinal two sections; the half was embedded in Tissue-Tec OCT compound (Sakura) and the other was embedded in paraffin. Paraffin sections were stained with H&E. The cryostat sections were subjected to immunochemical examinations with mAbs specific to CD4 (L3T4; BD Pharmingen) or CD8 (Ly-2; BD Pharmingen). Tumor area was measured by Macscope (Mitani). CD4- or CD8-positive cells were counted in total viable tumor area and peripheral stromal tissue within 0.5 mm from the margins of tumor tissue under the optical measure-assisted microscope.

Statistical analysis

All data were expressed as the mean ± SEM, and were analyzed by one-way ANOVA with Fisher's adjustment, except for animal survival. Survival was plotted using Kaplan-Meier curves and statistical relevance was determined using log-rank comparison. A probability value of $p < 0.05$ was considered significant.

Results

Transfection efficiency of SeV into mBM-DCs and their spontaneous activation

Immature mBM-DCs from BL/6 mice, propagated in the presence of GM-CSF and IL-4 for 7 days, were collected and transfected by SeV-luciferase or SeV-GFP for investigating gene transduction efficiency. As shown in Fig. 1*a*, *left panel*, dose-dependent luciferase expression was shown and the optimized expression was found around MOI = 40–100. Repeated FACS analyses for DCs transfected by SeV-GFP demonstrated that >90% of GFP-positive DCs were detected at more than MOI = 40, a finding representatively shown with forward scatter/side scatter (fsc/ssc) gating at MOI = 40 (Fig. 1*b*), therefore, all of the following experiments were performed at this titer as an optimal dose.

We next assessed the surface markers of DCs treated with SeV-expressing GFP or mIFN-β without any other stimulant, directly compared with a well-known strong but clinically irrelevant DC activator, LPS, at 2 μg/ml for 48 h of exposure, which had been shown to be the optimal dose for mDC activation in our preliminary data (data not shown). As shown in Fig. 1*c*, repeated FACS analyses showed that DCs treated with SeV-GFP or SeV-mIFN-β resulted in the high-level expression of the costimulatory molecules tested here, namely MHC class II, CD80, and CD86 molecules, which did not reach the level seen in the DCs treated with LPS. In comparison to their sharp expression patterns on LPS/DC, those seen on SeV-GFP or SeV-mIFN-β showed broad expression, suggesting the result of the broad expression of transgene seen in Fig. 1*b*. Other surface markers related to trafficking (CCR7) and adhesion (ICAM-1) were also up-regulated on DCs treated with SeV-GFP or SeV-mIFN-β which were nearly comparable to the level seen on LPS/DC. These results thus demonstrated that SeV could not only effectively transfer exogenous genes into DCs, but also spontaneously transform immature DCs to near fully activated mature DCs without other manipulation irrespective of the exogenous mIFN-β expression. In turn, LPS-activated DCs were seriously resistant to SeV-mediated gene transfer (usually <5%, data not shown).

To assess further phenotype of DCs activated by SeV, release of typical cytokines was examined by ELISA. As shown in Fig. 1*d*, up-regulation of type I IFN, e.g., IFN-β, was seen in DCs treated with SeV-GFP or SeV-mIFN-β, but not in immature DCs and LPS/DCs. In contrast, strongest expression of other cytokines tested, including Th1 cytokines (p70 subunit of IL-12 and IFN-γ), was seen in LPS/DCs.

Together with these results, SeV induces spontaneous maturation and activation of mBM-DCs, however, their phenotype is not equal to those seen in the treatment with LPS.

SeV/DC therapy induces complete elimination of B16F1 melanoma in vivo

Next, we asked whether DCs activated by SeV might have therapeutic potentials against an immune-competent murine melanoma model. We tested this by an early treatment regimen as follows.

First, to assess the effective route for antitumor activity of DC therapy, i.t., distant s.c., and i.v. (via tail vein, i.v.) injections of tumor lysate-pulsed DCs activated by SeV-GFP was started and

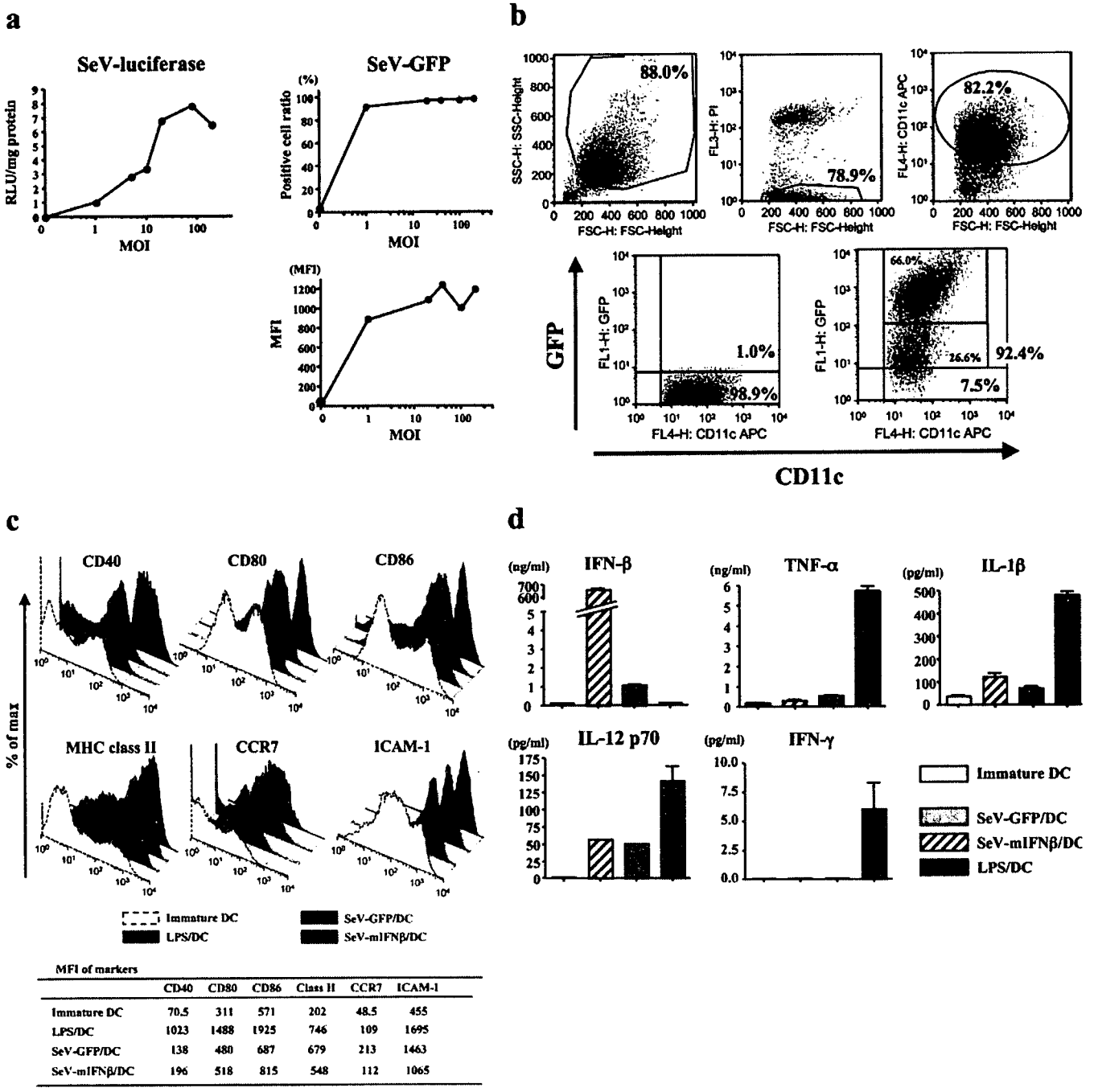

	CD40	CD80	CD86	Class II	CCR7	ICAM-1
Immature DC	70.5	311	571	202	48.5	455
LPS/DC	1023	1488	1925	746	109	1695
SeV-GFP/DC	138	480	687	679	213	1463
SeV-mIFNβ/DC	196	518	815	548	112	1065

FIGURE 1. Gene transfer efficiency of SeV to bone marrow-derived immature DCs and their spontaneous activation. Seven days after cultivation to generate immature DCs under IL-4 and GM-CSF, DCs were treated by SeV-luciferase or SeV-GFP. Forty-eight hours later, DCs were subjected to each analysis. Each experiment was done in triplicate or more and showed similar results. *a*, Quantitative optimization of dose-dependent gene expression efficiency using SeV-luciferase (*left graph*) and SeV-GFP (*upper right two graphs*: positive cell ratio, *bottom*: MFI, mean fluorescent intensity). Optimized expression was seen around MOI = 40–100. *b*, Scattered plots for fsc/ssc gating of DCs transfected with SeV-GFP at MOI = 40. Note 2 major populations of GFP-expressing DCs, GFP^{high} (66.0%) and GFP^{low} (26.6%) (*bottom right panel*). *c*, Expression level of activation markers (CD40, CD80, CD86, MHC class II) and Ags related to trafficking (CCR7) and to adhesion (ICAM-1) of DCs, treated with SeV-GFP, SeV-mIFN-β, or LPS (2 μg/ml). MFIs of each analysis were given below. *d*, Typical cytokine secretion from DCs treated with LPS, SeV-GFP, or SeV-mIFN-β. Immature DCs were used as negative control.

repeated three times every week 3 days after B16F1 (low malignant subline) cell inoculation. Efficient antitumor effect was only seen in the case of i.t. injection (Fig. 2*a*), a finding similar to the previous report by the other group in use of naive DCs (25). Therefore, the following experiments were done via the i.t. route.

Next, we directly compared the antitumor effect of i.t. administration of immature DC, LPS/DC/lysate, SeV-GFP/DC/lysate, and SeV-mIFN-β/DC/lysate by early treatment regimen indicated in Fig. 2*b*. In this study, we used immature DCs without tumor lysate as a control, because it has been known that ex vivo uptake of tumor Ag itself led DCs to activated state (26). Because B16 melanoma-burden mice were well-known to start to die around 2 wk after inoculation irrespective of tumor size, we here evaluated two more parameters, namely survival and the number of mice with eliminated tumor, to assess the beneficial effects of cancer vaccines.

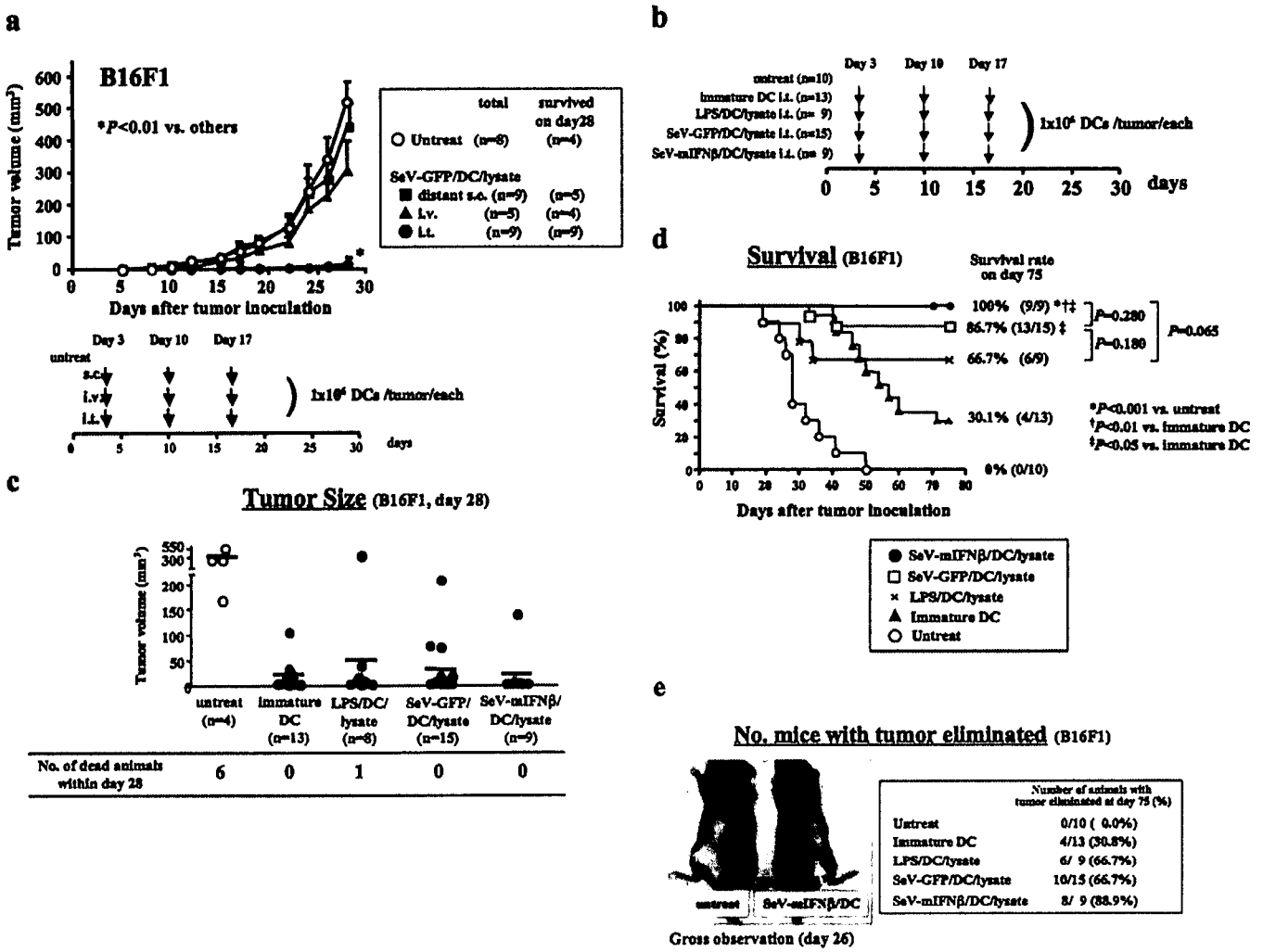

FIGURE 2. Assessment of antitumor activity of DCs modified by SeV against low-malignant murine melanoma B16F1. Three days after tumor cell inoculation, DCs were injected i.t. according to the indicated regimen (*a, bottom scheme*: early treatment regimen). Tumor lysate was pulsed to immature DCs which were subsequently treated with LPS, SeV-GFP, or SeV-mIFN-β, and these DCs were used for DC immunotherapy 8 h later. DC treatment was done three times. The data demonstrated were the total of three independent experiments. *a*, Time course of the tumor volume treated with SeV-GFP/DC/lysate via different administration routes (distant s.c.: s.c. injection, i.v.: i.v. injection via tail vein, and i.t.: intratumor injection). Numbers indicate tumor-bearing animals that survived over 28 days. *b*, Experimental design to assess the stimulator dependent antitumor effect of DCs. *c*, Dot plots indicating the tumor size of B16F1 melanoma following DC therapy. Numbers below indicate the dead animals within day 28. *d*, Survival curve of the mice bearing B16F1 melanoma treated with various DCs. Significant prolongation of survival was seen in SeV/DC groups. *e*, Typical and representative gross observation of mice with B16F1 tumors treated with or without SeV-mIFN-β/DC/lysate 26 days after tumor cell inoculation. Note complete rejection of tumors by SeV-mIFN-β/DC/lysate treatment (arrow), which was confirmed by histopathological examination (data not shown). Tumor rejection rate of mice at day 75 was also presented in the right column.

Tumor size. As shown in Fig. 2*c*, six animals of the untreated group and 1 of the LPS/DC/lysate group were dead within day 28. The tumor size on day 28 was efficiently disturbed by DC immunotherapy modified by SeV-GFP, SeV-mIFN-β, or LPS. However, a similar finding was also seen in the use of immature DCs, suggesting the results of spontaneous activation of DCs in vivo via i.t. route, as previously described by the other group (25).

In contrast, other parameters, survival, and tumor elimination ratio showed interesting results.

Survival. Significant prolongation of survival of animals was found only in groups of SeV-GFP/DC/lysate and SeV-mIFN-β/DC/lysate (Fig. 2*d*).

Number of mice with tumor eliminated. Ten of 14 mice (71.4%) treated with SeV-GFP/DC and 8 of 9 (88.9%) treated with SeV-mIFN-β/DC completely eliminated the tumor at day 75 (Fig. 2*e*), findings that were also confirmed microscopically (data not shown).

These results indicated that DC immunotherapy was beneficial for treating B16F1 melanoma in immune-competent mice, in views of survival and tumor elimination, and the therapeutic effects of DCs modified with SeV were equal or possibly more to that with strong DC activator LPS, an effect that was significantly improved by exogenous IFN-β expression.

Limited responses of mIFN-β protein as well as mIFN-β gene therapies on highly malignant and less immunogenic B16F10 melanoma in vivo

Direct efficacy evaluation demonstrated in Fig. 2 suggests the potential use of SeV-mediated modification of DC functions for cancer immunotherapy; however, significant and clear improvement over LPS/DC was not found. Furthermore, immature DCs showed significant reduction of tumor size, suggesting that the tumor model of low malignant B16F1 melanoma was not appropriate to evaluate the potentials of SeV/DCs. Therefore, we next tried to

treat a highly malignant and less immunogenic subtype of B16 melanoma, namely B16F10, using SeV/DCs. Before this trial, we first assessed the biological effects of mIFN-β in vitro and of protein and gene therapy with mIFN-β in vivo.

As shown in Fig. 3*a*, mild and dose-dependent growth inhibition was seen in B16F1 cells in vitro, and the effect was more pronounced in B16F10 cells, indicating that B16 melanomas are sensitive to IFN-β, similar to findings in clinical settings (27). In contrast, murine hepatocellular carcinoma, MH134, was not apparently sensitive to IFN-β (Fig. 3*a*).

Next, we treated B16F10 tumors in vivo with mIFN-β protein, which has been a standard clinical therapeutic, as well as with SeV-mIFNβ as a gene therapy, by a treatment regimen beginning at a later stage of tumor development (tumor diameter = 7–9 mm). As shown in Fig. 3*b*, both treatments tended to delay the growth of the B16F10 tumors; however, the tumor volume had relapsed by about day 30. The relapse of tumor growth was likely due to withdrawal of the local concentration of mIFN-β, because in vivo expression of SeV-mediated gene transfer has been shown to be transient (11).

These findings suggest that protein and gene therapies by mIFN-β contributed to the suppression of tumor growth of B16F10 tumors in vitro and in vivo; however, the effect was not

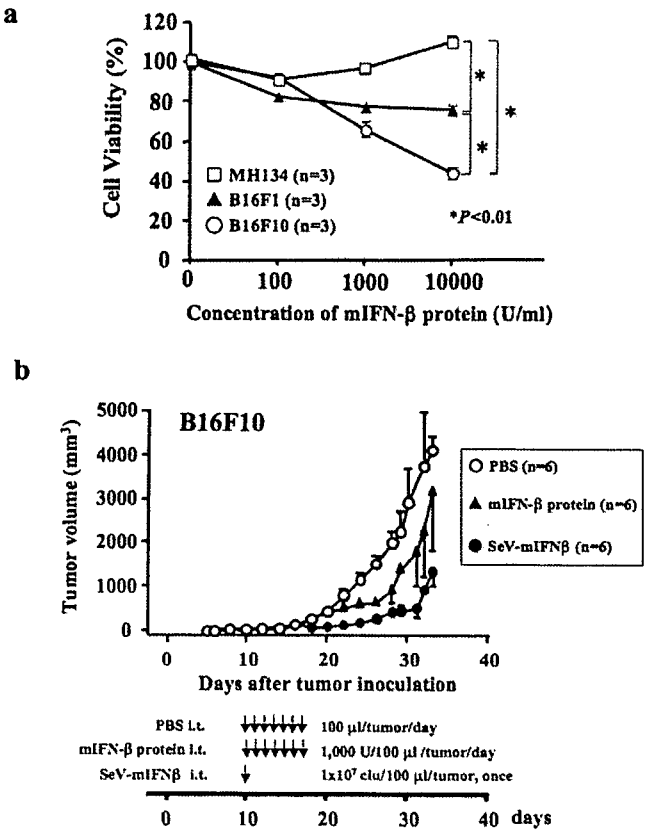

FIGURE 3. Antitumor activity of murine IFN-β against murine tumor cells in vitro (*a*) and in vivo (*b*). *a*, In vitro cytotoxicity of mIFN-β to murine melanomas (lower malignancy, B16F1; higher malignancy, B16F10) and a hepatocellular carcinoma (MH134). After 48-h culturing in the presence of mIFN-β protein, cell viability was assessed. The viability of MH134 (□) was not affected by mIFN-β, and in contrast, melanomas were sensitive to mIFN-β, suggested by the observed dose-dependent effects. Note that B16F10 (○) was more sensitive than B16F1(▲) to mIFN-β. *b*, Antitumor activity of protein (▲) and gene (●) therapies of mIFN-β in vivo. Ten days after tumor cell inoculation, when the established tumor was well-vascularized, protein or gene therapy was started according to the indicated regimen (*b*, bottom scheme: late treatment regimen).

sufficient to control a highly malignant cell type, even though the tumor cells are sensitive to mIFN-β. This could be explained because the duration of local concentration of mIFN-β might not be sufficient to show the long-lasting antitumor effect.

Modulation of antitumor effects and immune responses to IFN-β-sensitive, established tumors by SeV/DCs expressing mIFN-β

Antitumor effect. IFN-β is known to be an antitumor cytokine via multiple mechanisms, including a direct antiproliferative effect, enhancement of NK cell activity, and up-regulation of tumor Ag and MHC class I and II (28). Therefore, we next asked whether DC therapy modulated by exogenous *mIFN-β* genes might affect the antitumor effect as well as immune responses against B16F10 melanoma.

First, we assessed MHC class I expression and its modulation by mIFN-β by flow cytometry analyses, because it is well-known that the expression of this molecule on tumor cells is required to be recognized by antitumor CTLs induced by cancer immunotherapy (29). As shown in Fig. 4*a*, the baseline expression of MHC class I ($H\text{-}2^k$) was high, and the level was not significantly changed by the treatment with mIFN-β. In contrast, both B16F1 and B16F10 cells expressed a very low level of MHC class I ($H\text{-}2^b$) at baseline, and after 48 h of culturing in the presence of 1000 U/ml mIFN-β protein, the level of MHC class I was dramatically increased. Together with Fig. 3*a*, these results might suggest that SeV/DCs expressing mIFN-β possibly enhanced the antitumor effect seen in the use of sole SeV/DCs.

To test this possibility, we next evaluated the antitumor effect SeV-mIFN-β/DCs, directly compared with those of LPS/DCs and SeV-GFP/DCs using established MH134 and B16F10 melanoma in vivo via later treatment regimen.

MH134 tumor

Tumor size (Fig. 4b). As expected, the tumor growth of established MH134 tumors was markedly inhibited irrespective of the types of DCs, namely, LPS/DCs, SeV-GFP/DCs, and SeV-mIFN-β/DCs, by the later treatment regimen (Fig. 4*b*).

Survival. No animal bearing MH134 was dead during experimental course.

Number of mice with tumor eliminated. No animal showed elimination of tumor irrespective of treatments.

B16F10 tumor

Tumor size (Fig. 4c). Evaluation of tumor size was relatively difficult, because 40% and all of untreated animals were dead within days 20 and 36, respectively (Fig. 4*c*, *upper panel*). In addition, death of animals was not corresponded to the size of tumor.

Survival. Although DC/lysate and LPS/DCs were likely to inhibit the growth of B16F10 tumors in vivo (Fig. 4*c*), both treatments did not contribute to the significant prolongation of the survival (Fig. 4*d*). In contrast, significant prolongation of survival over day 50 and tumor dormancy of animals bearing B16F10 melanoma were observed only in SeV/DC groups. A beneficial effect of the *IFN-β* transgene was seen in tumor size which was evaluated on day 50 (Fig. 4*e*).

Number of mice with tumor eliminated. No animal showed elimination of tumor irrespective of treatments.

Together, these results indicate that modification of the function of DCs by SeV expressing mIFN-β dramatically enhances the antitumor effect to tumor cells that are sensitive to IFN-β. Furthermore, these results strongly suggested that the modification of DC functions by SeV was beneficial on the survival, and exogenous IFN-β mainly contributes to the reduction of tumor volume.